Drug Design, Development and Therapy

Dovepress
Taylor & Francis Group

Open Access Full Text Article

ORIGINAL RESEARCH

Exploring the Therapeutic and Gut Microbiota-Modulating Effects of Qingreliangxuefang on IMQ-Induced Psoriasis

Zhengyao Yu[1–5,*], Yingying Wang[2,3,6,*], Yingxue Guo[2,3,6], Ruotong Zhu[1,4], Yimiao Fang[1], Qinghua Yao[7], Huiying Fu[2,3,5,6], Ang Zhou[8], Lili Ma[1], Qiyang Shou[2,3,5,6]

[1]The First Affiliated Hospital of Zhejiang Chinese Medical University (Zhejiang Provincial Hospital of Traditional Chinese Medicine), Hangzhou, Zhejiang, 310006, People's Republic of China; [2]The Second School of Clinical Medicine, Zhejiang Chinese Medical University, Hangzhou, Zhejiang, 310053, People's Republic of China; [3]Jinhua Academy, Zhejiang Chinese Medical University, Hangzhou, Zhejiang, 310053, People's Republic of China; [4]The First School of Clinical Medicine, Zhejiang Chinese Medical University, Hangzhou, Zhejiang, 310053, People's Republic of China; [5]Yongkang Hospital of Traditional Chinese Medicine, Jinhua, Zhejiang, 321300, People's Republic of China; [6]School of Pharmaceutical Sciences, Zhejiang Chinese Medical University, Hangzhou, Zhejiang, 310053, People's Republic of China; [7]The Second Affiliated Hospital of Zhejiang Chinese Medical University, Xinhua Hospital of Zhejiang Province, Hangzhou, Zhejiang, 310005, People's Republic of China; [8]Department of Dermatology, Yiwu Central Hospital Medical Community Choujiang Hospital District, Yiwu, Zhejiang, 322000, People's Republic of China

*These authors contributed equally to this work

Correspondence: Lili Ma, The First Affiliated Hospital of Zhejiang Chinese Medical University (Zhejiang Provincial Hospital of Traditional Chinese Medicine), Hangzhou, Zhejiang, 310006, People's Republic of China, Email lilyma163@163.com; Qiyang Shou, The Second School of Clinical Medicine, Zhejiang Chinese Medical University, Hangzhou, Zhejiang, 310053, People's Republic of China, Email sqy133@126.com

Purpose: To investigate the therapeutic and gut microbiota-modulating effects of Qingreliangxuefang (QRLXF) on psoriasis.

Materials and Methods: We used network pharmacology, a computational approach, to identify key bioactive compounds and biological targets, and explored the molecular mechanisms of QRLXF. The effects of QRLXF on keratinocyte proliferation and inflammation were evaluated using a mouse model of psoriasis. Changes in the gut microbiota were analyzed via 16SrDNA sequencing, and T cell subsets were assessed using flow cytometry.

Results: Network pharmacology analysis suggested that QRLXF ameliorated psoriasis by modulating Th17 cell differentiation. Further experiments confirmed the anti-inflammatory effects and relief of psoriatic lesions in IMQ-induced mice. 16SrDNA sequencing revealed significant shifts in the gut microbiota, notably increases in Ligilactobacillus and Lactobacillus genera and decreases in Anaerotruncus, Negativibacillus, Bilophila, and Mucispirillum, suggesting a potential relationship between specific microbiota changes and Th17 cell differentiation.

Conclusion: QRLXF alleviated psoriatic dermatitis by regulating Th17 cell responses and modifying gut microbiota profiles, highlighting its therapeutic potential for psoriasis treatment.

Plain Language Summary: Psoriasis affects millions globally. We studied a traditional herbal formula, Qingreliangxuefang (QRLXF), for its potential in treating psoriasis. Using computer tools, we found QRLXF may control Th17 cells, which play a role in psoriasis. Testing QRLXF in mice with psoriasis-like skin issues showed reduced inflammation and improved skin appearance. Gut bacteria analysis revealed more beneficial bacteria like Ligilactobacillus and Lactobacillus and fewer harmful ones. Our findings suggest QRLXF could be a promising new treatment option for psoriasis.

Keywords: psoriasis, QRLXF, T cell differentiation, 16SrDNA sequencing, Th17 cell responses

Introduction

Psoriasis is an immune-mediated skin disorder marked by erythema, scaling, and skin thickening, driven by an interaction of genetic factors and various external triggers.[1] The prevalence of psoriasis varies significantly across

Received: 8 September 2024
Accepted: 24 March 2025
Published: 28 April 2025

Graphical Abstract

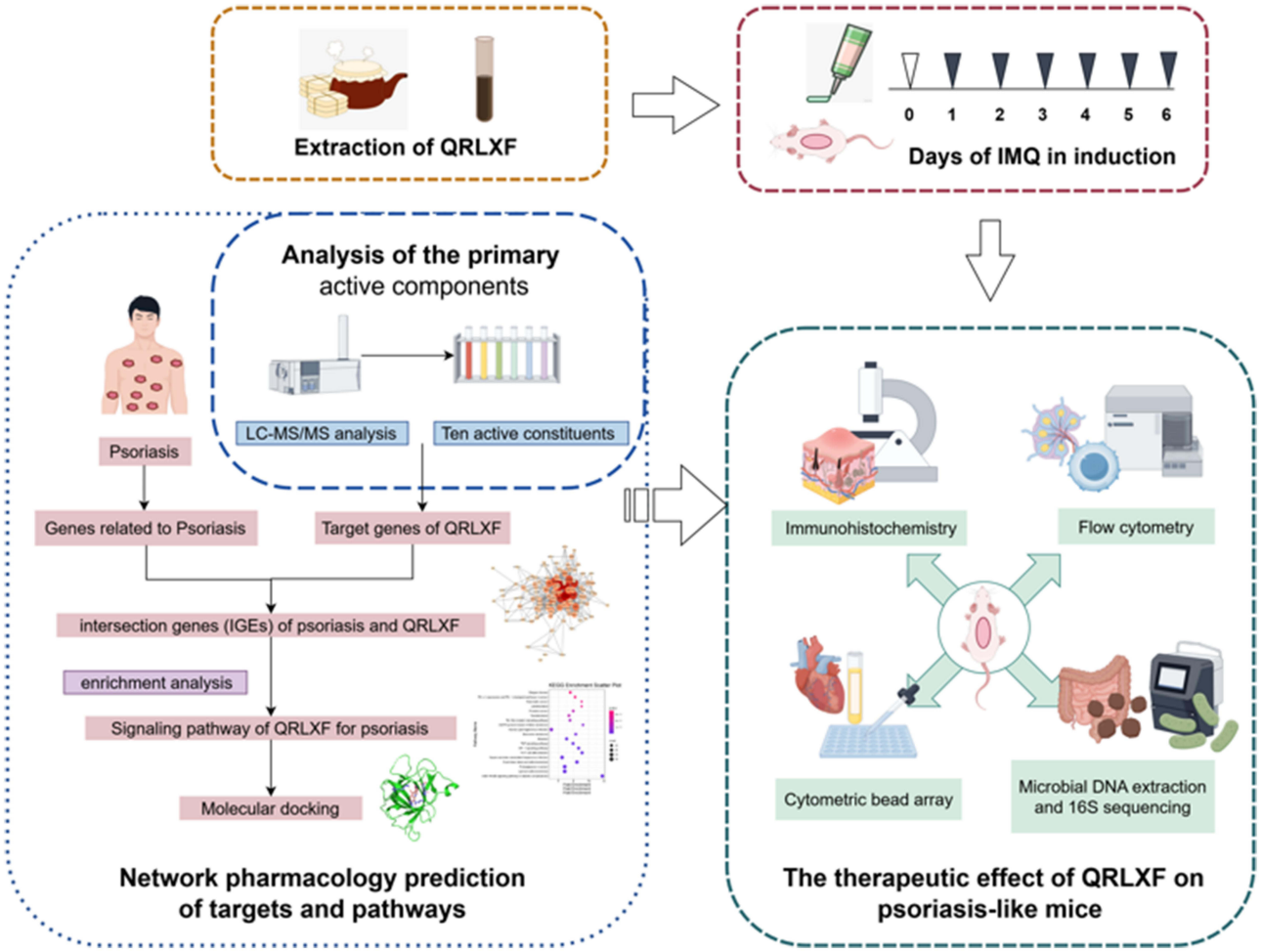

countries, but China has the largest number of affected adults globally due to its population size.[2,3] According to the 2021 Global Burden of Disease (GBD) study, the age-standardized incidence rate (ASIR) of psoriasis in China is 59.70/100,000, while the age-standardized prevalence rate (ASPR) is 474.02/100,000, imposing a substantial burden on healthcare systems and society.[4] Various psoriasis treatments exist, including topical corticosteroids, phototherapy, and systemic medications such as methotrexate and cyclosporine.[5] Biologic therapy targets precise inflammatory factors, demonstrating notable efficacy.[6,7] However, potential side effects persist during treatment, including liver toxicity, heightened infection risk, diminished efficacy, and possible immune drift.[8] Concurrently, the chronic nature of psoriasis imposes financial burdens on patients, eliciting additional concerns and anxieties.[9] Consequently, identifying safe, cost-effective, and efficacious treatments for psoriasis holds considerable importance.

The pathogenesis of psoriasis is characterised by the persistent activation of various immune cells, resulting in inflammation.[10,11] In the pathogenesis of psoriasis, a central role is played by Th17 cells, as the generation of IL-17 serves as a critical factor in sustaining chronic inflammatory responses.[12,13] However, the precise mechanisms underlying psoriasis pathogenesis remain incompletely understood. Recent studies have demonstrated that psoriasis patients experience gut microbiota dysbiosis, with lower levels of probiotics and higher amounts of pro-inflammatory bacteria in their gut microbiota.[14–17] Moreover, findings indicate that those with psoriasis display an imbalance in the Firmicutes/

Bacteroides (F/B) ratio, which impacts the production of intestinal short-chain fatty acids (SCFAs).[16,18] Abnormal metabolites stimulate the proliferation of intestinal macrophages, thereby impacting gut immunity.[19]

The concept of the gut-microbiota-skin axis further elucidates the role of the microbiota in skin diseases from an immunological perspective.[20] The gastrointestinal tract serves as a crucial site for the regulation of Th17 cell proliferation and differentiation.[21] The gut microbiome can influence epithelial barrier function and immune cell differentiation, playing a pivotal role in various inter-organ communication processes.[22,23] Alterations in gut microbiota homeostasis and its metabolites drive the differentiation of Th17 cells in the colonic lamina propria, contributing to systemic inflammation in genetically predisposed individuals.[24–26] Studies have shown that segmented filamentous bacteria (SFB) can promote systemic Th17 cell proliferation upon intestinal colonization, exacerbating autoimmune diseases such as lupus nephritis[27] and autoimmune arthritis.[28] Conversely, antibiotics such as penicillin administered at appropriate doses can modulate bacterial populations, reduce Th17 cells in the small intestinal lamina propria, and reduce inflammatory bowel disease susceptibility in mice.[29] Similar effects have been observed in skin diseases. Studies have shown that germ-free and broad-spectrum antibiotic-treated mice exhibit reduced local and systemic Th17 activation when induced by imiquimod.[30,31] Moreover,faecal transplantation experiments demonstrated that faeces from patients with severe psoriasis worsen skin inflammation and increase Th17 cell differentiation in mice.[32] Thus suggests that the gut microbiota influences psoriasis development by modulating Th17 cell-mediated immune responses.

Traditional Chinese Medicine (TCM) is frequently used in the clinical treatment of psoriasis because of its rapid efficacy, low cost, and capacity to prevent relapse. Blood-heat syndrome is the most common type of psoriasis observed during the active phase. Qingreliangxuefang (QRLXF), a Chinese medicine compound prescription, exerts therapeutic effects through heat clearing, blood cooling, detoxification, and dehumidification. However, the mechanisms underlying these effects require further investigations. Studies have confirmed that the constituents of QRLXF, including Scutellariae Radix,[33,34] Smilacis Glabrae Rhizoma,[35,36] and Curcumae Radix,[37–39] exhibit favourable therapeutic outcomes in psoriasis treatment and hold promise for modulating the gut microbiota. In clinical settings, compound formulations are extensively used in TCM, offering a holistic therapeutic impact, catering to a wide patient demographic range, and having significant practical utility. The intestinal microbiota is a crucial target for therapeutic intervention with TCM compounds.[40] Nevertheless, the intricate nature of drug composition and structure presents challenges for advancing research in this area.

The purpose of this study was to evaluate the efficacy of QRLXF in the treatment of psoriasis and explore its underlying mechanism. We used network pharmacology to make preliminary predictions and experimentally verify these mechanisms. In addition, we used 16S rDNA technology to investigate whether the therapeutic effects of QRLXF on psoriasis were related to the regulation of intestinal flora.

Materials and Methods

Preparation of Qingreliangxuefang Extract (QRLXF)

Qingreliangxuefang includes 11 Chinese herbs: Bubali Cornu, Herba Solani Lyrati, Isatidis Folium, Curcumae Radix, Rehmanniae Radix, Moutan Cortex, Smilacis Glabrae Rhizoma, Scutellariae Radix, Sophorae Flos, Rhei Radix Et Rhizoma, and Arnebiae Radix. These herbs were supplied by Zhejiang Hospital of Traditional Chinese Medicine (Hangzhou, China). These herbs were soaked in purified water (1:10, w/v) for 30 min to allow the active ingredients to fully dissolve in the decoction. Bubali Cornu was removed and decocted separately for approximately 3 h. Subsequently, other herbs were added to the pots and boiled. After boiling, the mixture was simmered under low heat for 30 min, and the decoction was collected. This process was repeated using the same volume of purified water as the first time. The two batches of decoction were then combined, concentrated under reduced pressure, freeze-dried into powder, and stored at –40 °C.

UHPLC-OE-MS and HPLC Analysis of QRLXF

Sample 20mL was taken for Ultra High-Performance Liquid Chromatography - Orbitrap Exploris - Mass Spectrometry (UHPLC-OE-MS) to further clarify the composition of QRLXF. The analysis was conducted using a UHPLC system (Vanquish, Thermo Fisher Scientific) equipped with the Phenomenex Kinetex C18 (2.1 mm × 100 mm, 2.6 μm) and the

Orbitrap Exploris 120 mass spectrometer (Orbitrap MS, Thermo). The mobile phase (A: 0.01% acetic acid in water; B: Isopropanol (IPA): Acetonitrile (ACN) (1:1, v/v)) was delivered at a speed of 0.3 mL/min: 0–1 min (1%B); 1–8 min (1%–99% B); 8–9 min (99%B) and 9–12 min (1% B). Under the control of the acquisition software (Xcalibur, Thermo), MS/MS spectra were acquired using the information-dependent acquisition (IDA) mode of an Orbitrap Exploris 120 mass spectrometer. The original data were processed and converted into the mzXML format using ProteoWizard. We then used the BiotreeDB (V3.0) and the R software to identify the metabolites.

The specific contents of the active components were further quantified using HPLC, and standard references for "hypoxanthine, luteolin, indirubin, curdione, catalpol, paeoniflorin, astilbin, baicalin, kaempferol, and rhein" were purchased from Shanghai Yuanye Biotechnology Co. Ltd. Each sample was dissolved in 50% methanol to prepare 1 mg/mL stock solutions. A 2.5-mL aliquot of each solution was combined in a 50 mL volumetric flask and diluted with methanol to prepare a 50 μg/mL mixed stock solution. This solution was further diluted with methanol to obtain working solutions of 1.0, 2.0, 5.0, 10.0, 25.0, and 50.0 μg/mL. The herbal decoction (1.48 g/mL) was mixed with 6–9 mL of 80% methanol, vortexed, and ultrasonically extracted for 20 min. After cooling, the mixture was diluted with 80% methanol, centrifuged if necessary, and filtered through a 0.45-μm membrane. The filtrate was used as the sample solution.

The compounds in QRLXF were analyzed using an Agilent 1260 HPLC system equipped with a Kromasil 100-5-C18 column (4.6 mm × 250 mm, 5 μm). The mobile phase consisted of solvent A (0.1% phosphoric acid aqueous solution) and solvent B (methanol), with a gradient elution as follows: 0–30 min, 10%–30% B; 30–50 min, 30%–60% B; and 50–65 min, 60%–100% B. The flow rate was 1.0 mL/min, column temperature was 26°C, and detection was done at 210 nm with a 10 μL injection volume.

Construction of Candidate Active Molecules and Potential Targets Database

The potential targets of the active components in QRLXF were determined using the TCMSP database (https://old.tcmsp-e.com/tcmsp.ph), PharmMapper (http://www.lilab-ecust.cn/pharmmapper/), BATMAN-TCM (http://bionet.ncpsb.org.cn/batman-tcm/index.php), and Swiss Target Prediction (http://www.swisstargetprediction.ch/index.php). Relevant literature was reviewed to verify their active ingredients. Through GeneCards (https://www.genecards.org/), DrugBank (https://www.drugbank.com/), TTD (http://db.idrblab.net/ttd/), DisGenet (https://www.disgenet.org/), and OMIM (https://omim.org/), genes related to psoriasis were identified. An online data analysis website (https://www.bioinformatics.com.cn/static/others/jvenn/example.html) was used to identify the intersection genes (IGEs) of psoriasis and QRLXF, which were visualized using a Venn diagram.

Protein–Protein Interaction (PPI) Network Construction and Enrichment Analysis

The STRING online database (http://string-db.org) was used to generate a PPI network of the IGEs. We then imported the resulting network data into Cytoscape (version 3.10) for visualisation. By filtering values such as degree, betweenness, and closeness, the effective components and targets were analyzed, and hubs were extracted to construct the network topology diagram.

To comprehensively assess the functions of QRLXF in psoriasis treatment, enrichment analysis was conducted using IGEs. Gene Ontology (GO) enrichment was performed using the DAVID database (http://david.abcc.ncifcrf.gov), including cellular components, molecular functions, and biological processes ($P < 0.05$).To explore the biological roles of these functional targets, KEGG pathway enrichment analysis was performed. The top 20 pathway terms were identified as significantly annotated ($P < 0.01$). Finally, access to QRLXF may affect the pathways associated with psoriasis.The results were visualised using an online bioinformatics website (https://www.bioinformatics.com.cn/).

Molecular Docking and Visualization

Seven prospective therapeutic targets were identified by combining the results of the PPI network's topological analysis with literature analysis. The key QRLXF compounds in mol2 format were downloaded from the TCMSP database and converted to pdbqt format using AutoDockTools 1.5.6. The 3D structure of the target was obtained from the PDB database (https://www.rcsb.org). The PyMOL software and AutoDockTools 1.5.6 were used to remove all ligands and water molecules, followed by hydrogenation, and the results were finally saved in the pdbqt format. The pdbqt file of the target and ligand was molecularly docked, and the results were visualised using the PyMOL software.

Animals and Ethics Statement

Female SPF-grade FVB/NJ mice were obtained from the Animal Experimental Research Center of Zhejiang Chinese Medical University. The weights of the mice ranged between 18–22 g, and they were randomly assigned to five groups, with six mice in each group. The groups included the control, model (IMQ), QRLXF-L (19.5 g/kg), QRLXF-H (39 g/kg), and positive control (MTX, 1 mg/kg). Daily oral gavage was performed, and the model (IMQ) and control groups were administered distilled water. The QRLXF-L and QRLXF-H groups received 19.5 g/kg or 39 g/kg QRLXF, which were dissolved in distilled water. The positive control (MTX) group was administered MTX (1 mg/kg). Furthermore, 62.5 mg of 5% imiquimod cream was applied daily to the depilated back areas of the mice for 6 consecutive days, except in the control group. Erythema, skin crust, and infiltration in the mice were monitored dynamically and evaluated using the Psoriasis Area and Severity Index (PASI) score. At the end of the study, the mice were euthanised. Blood, spleen, lymph nodes, and dorsal skin samples were collected for further analyses. This study was approved by the Animal Ethical and Welfare Committee of ZCMU (IACUC-20240415-01). All experiments were performed in accordance with the National Institutes of Health Guide for the Care and Use of Laboratory Animals (NIH Publications No. 8023, revised 2011).

Histological and Immunohistochemical Analysis

The skin lesions were fixed in 4% paraformaldehyde. The fixed skin was embedded in paraffin and then sectioned into 4 μm-thick slices to be stained with haematoxylin and eosin (H&E). Three visual fields per section were captured, and the thickness and number of epidermal cell layers were measured using digital pathological scanning software (NDP View 2U12388-01, Hamamatsu, Japan). Immunohistochemical (IHC) assays were also performed. Paraffin sections were first incubated with anti-PCNA monoclonal antibodies overnight, and then with HRP-conjugated goat anti-rabbit IgG (Servicebio, Wuhan, China) for 50 min at room temperature. The sections were stained with haematoxylin and DAB (Servicebio, Wuhan, China). The PCNA-positive cells were observed under a microscope using the ImageJ software version 1.8.0 and a NanoZoomer digital pathology scanner (Nikon, Tokyo, Japan).

Cytometric Bead Array

Cardiac blood was collected from the mice in each group. The blood was coagulated for 2 h at room temperature and centrifuged at 3500 rpm for 15 min, then 200 μL of serum was collected. After freeze-drying at –40 °C, the serum was reconstituted in 20 μL of sample diluent. The skin lesion tissues were weighed, cut into small pieces, and homogenised in a 1:9 ratio of tissue weight to PBS volume. After centrifuging the homogenate for 10 minutes at 4°C at 4000 rpm, the supernatant was collected. The Mouse CBA Kit (BD Biosciences, San Jose, CA, USA) was used to assess the amounts of IL-17A, IL-2, IL-4, IL-6, TNF, and IFN-γ in both serum and skin tissues.

Flow Cytometry

The spleens and the skin-draining lymph nodes of the mice were collected, ground, filtered, and centrifuged to obtain a single-cell solution. The cells were labelled with surface markers using antibodies including anti-CD4-FITC, anti-CD3e-BV605, anti-NK1.1-BV421, anti-CD25-BV605, and anti-CD8-APC-H7. The cells were fixed and permeabilized using a transcription factor buffer kit (BD Biosciences, San Diego, USA). Then, intracellular labelling was performed using anti-T-bet-BV421, anti-GATA-3-PerCP-Cy5.5, anti-RORγT-APC, and anti-Foxp3-PE antibodies. All antibodies were purchased from BD Pharmingen, Biosciences, or Horizon. A FACS Canto II flow cytometer (BD Biosciences) was used to collect and analyse the data.

Microbial DNA Extraction and 16S Sequencing

Colon contents were collected after the mice were euthanised, and total DNA was extracted using a QIAamp Fecal DNA Kit (Qiagen). PCR amplification was performed with primers 341F (5'-cctacgggnggcwgca3') and 805R (5'-GACTACHVGGGTATCTAATCC-3'). After validation by 2% agarose gel electrophoresis and purification using AMPure XT beads (Beckman Coulter Genomics, USA), the products were quantified using a Qubit fluorometer (Invitrogen, USA). Amplicons were pooled based on their concentration of the PCR amplicon and sequenced on an Illumina NovaSeq 6000

platform using a 2×250 bp back-end sequencing model. After assigning paired-end reads, the barcodes and primer sequences were truncated using Cutadapt (v1.9) and merged into longer reads based on overlap using FLASH (version 1.2.8). We used fqtrim (version 0.94) for a high-quality scanning of the original reading to obtain a clean label. Chimeric sequences were filtered using the Vsearch software (version 2.3.4). After further processing with the QIIME2 software, the characteristic sequence and abundance table of the amplicon sequence variant (ASV) were obtained. Based on this, diversity evaluations were carried out, including α-diversity and β-diversity analysis. The SILVA's NT-16s database (https://www.arb-silva.de/documentation/release138/) was used to assign ASV species according to their characteristics with a confidence threshold of 0.7. The R package (version 3.4.4) was used to generate additional diagrams.

Statistical Analysis

GraphPad Prism 9 (San Diego, CA, USA) and IBM SPSS 25.0 (Chicago, IL, USA) were used for data analysis. Results were presented as mean±SD. One-way ANOVA was used to analyse the multivariate data. Statistical significance was set at $p < 0.05$.

Results

Analysis and Quantification of the Primary Bioactive Components in QRLXF

The components of QRLXF were analyzed by UHPLC-OE-MS. Positive (Figure 1A) and negative (Figure 1B) flow diagrams of QRLXF are presented. After being validated through literature analysis, the primary constituents of QRLXF have been identified as hypoxanthine, luteolin, indirubin, curdione, catalpol, paeoniflorin, astilbin, baicalin, kaempferol, and rhein (Table 1). Subsequently, 4 major components of QRLXF, namely hypoxanthine, astilbin, baicalin, and rhein, were further identified using HPLC (Figure 1C). The concentrations of these components in QRLXF are shown in Table 2.

Preliminary Study on the Mechanism of Action of QRLXF on Psoriasis

We used network pharmacology and molecular docking to predict the mechanism of action of QRLXF in the treatment of psoriasis.The 4 major components of QRLXF were identified through LC-MS/MS analysis and subsequently confirmed by a review of the literature. A total of 656 potential targets of these active ingredients were identified from the PharmMapper, TCMSP, BATMAN-TCM, and SwissTargetPrediction databases. A drug-component-target network was built based on these constituents (Figure 2A). Targets related to "psoriasis" were sourced from multiple databases, including TTD, OMIM, GeneCards, DisGeNET, and DrugBank. Genes with a high frequency of association ($n \geq 2$) were identified across the various disease databases, leading to the identification of 1,072 key targets (Figure 2B). A Venn diagram of the QRLXF constituent-related and psoriasis-related targets revealed 161 common genes (Figure 2C). These 161 targets were entered into a PPI network using the STRING database. Topological characteristics were analyzed using Cytoscape 3.7.0, and hub networks were identified using CytoNCA. The top 23 targets associated with QRLXF treatment for psoriasis were identified by filtering values such as degree, betweenness centrality (BC), and closeness centrality (CC). These targets include TGFβ1, HSP90AA1, JUN, STAT1, IL-2 and IL1β (Figure 2D). The KEGG pathway and GO annotations of the 161 intersecting target proteins were further analyzed using the DAVID database. GO enrichment analysis identified biological processes associated with psoriasis, primarily involving responses to inflammatory, lipopolysaccharide, and xenobiotic stimuli (Figure 2E). Furthermore, KEGG enrichment analysis suggested that QRLXF might mitigate abnormal immune responses in psoriasis by modulating pathways such as the TNF signalling pathway and the Th17 cell differentiation (Figure 2F).

To validate the results of our network pharmacological analysis, we used molecular docking to evaluate the association between key compounds and therapeutic targets. Binding energies smaller than −4.25 kcal. mol^{-1} are thought to indicate ligand activity with the receptor. A binding energy less than −5.0 $kcal.mol^{-1}$ implies moderate binding activity, while a binding energy less than −7.0 $kcal.mol^{-1}$ suggests high binding activity. The docking-binding energies are shown in Figure 3B. We use IL-2 and IL1β as examples to visualise the docking results (Figure 3A).

QRLXF Alleviates Psoriasis-Like Skin Symptoms in IMQ-Induced Mice

To investigate the protective effects of QRLXF, psoriasis-like skin lesions were induced. As shown in Figure 4A, compared to the control mice, the model mice showed obvious scales and erythema on the back. Meanwhile, QRLXF

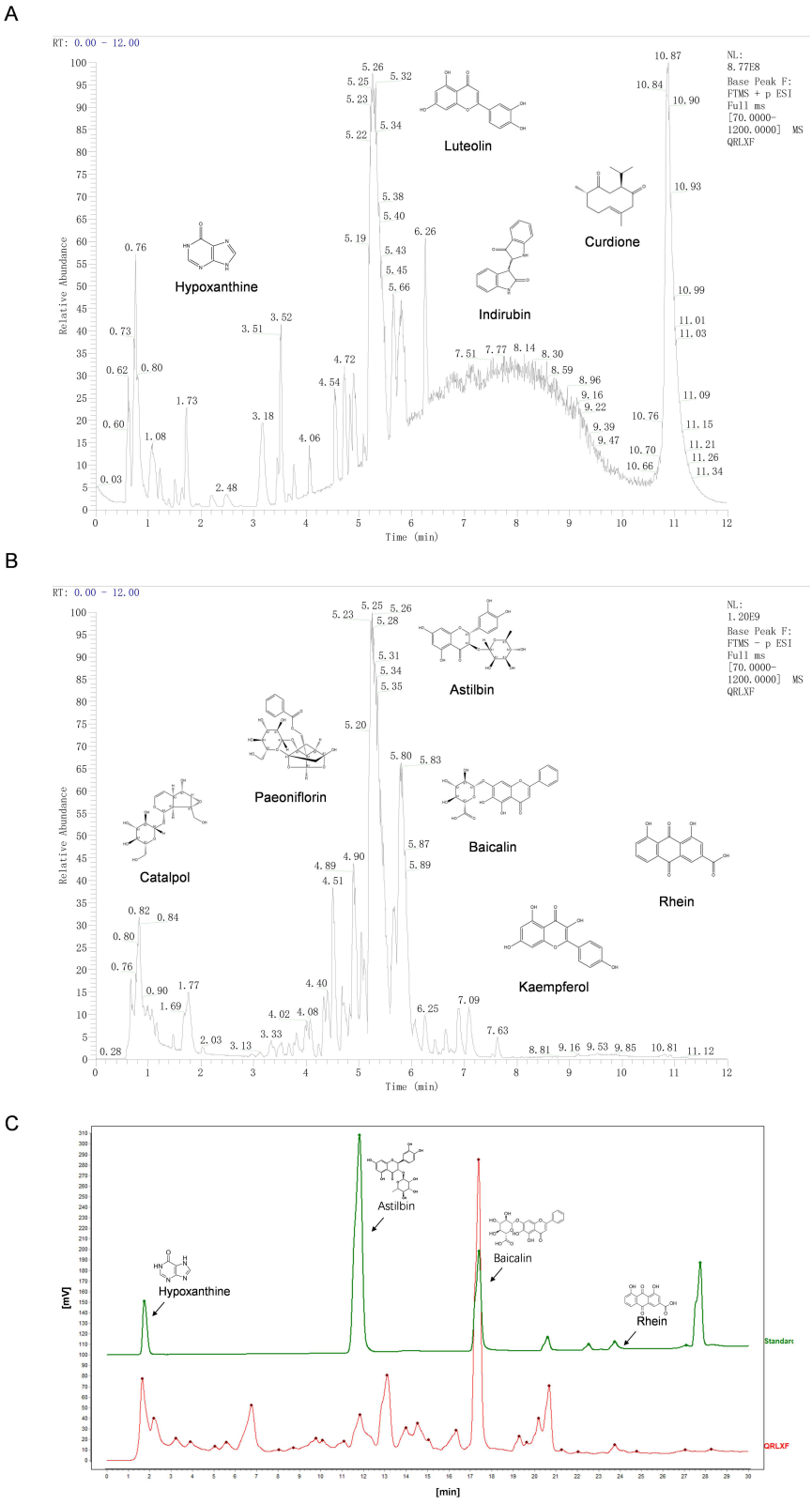

Figure 1 Identification of main chemical components in QRLXF by UHPLC-OE-MS and HPLC analysis. (**A**) Positive ion total ion current of QRLXF methanol extract; (**B**) Negative ion total ion current of QRLXF methanol extract; (**C**) HPLC analysis of QRLXF and its four standard compounds.

https://doi.org/10.2147/DDDT.S492044

Table 1 UHPLC-OE-MS identification results of QRLXF chemical components

NO	Compound Name	Formula	Type	mzmed	rtmed	Precursor Type	Pubchem ID	Origin
1	Hypoxanthine	C5H4N4O	POS	137.045	75.7	[M+H]+	790	Bubali Cornu
2	Luteolin	C15H10O6	POS	287.054	402.4	[M+H]+	5280445	Herba Solani Lyrati
3	Indirubin	C16H10N2O2	POS	263.081	429.2	[M+H]+	10177	Isatidis Folium
4	Curdione	C15H24O2	POS	237.184	430.8	[M+H]+	166874	Curcumae Radix
5	Catalpol	C15H22O10	NEG	361.113	86.6	[M-H]-	91520	Rehmanniae Radix
6	Paeoniflorin	C23H28O11	NEG	479.155	273.1	[M-H]-	442534	Moutan Cortex
7	Astilbin	C21H22O11	NEG	449.108	303.5	[M-H]-	119258	Smilacis Glabrae Rhizoma
8	Baicalin	C21H18O11	NEG	445.076	315.4	[M-H]-	64982	Scutellariae Radix
9	Kaempferol	C15H10O6	NEG	285.04	368.8	[M-H]-	5280863	Sophorae Flos
10	Rhein	C15H8O6	NEG	283.024	413.9	[M-H]-	10168	Rhei Radix Et Rhizoma

Table 2 Concentrations of 4 Major Compounds in QRLXF

Compound	Content (mg/g)
Hypoxanthine	0.261
Astilbin	0.069
Baicalin	0.767
Rhein	0.149

Abbreviations: 16SrDNA, 16S ribosomal DNA; ACN, Acetonitrile; ASIR, age-standardized incidence rate; ASPR, age-standardized prevalence rate; ASV, amplicon sequence variant; BC, betweenness centrality; CC, closeness centrality; DAO, diamine oxidase; DAB, 3.3'-Diaminobenzidine; F/B, Firmicutes/Bacteroides; GBD, Global Burden of Disease; GO, gene ontology; H&E, hematoxylin and eosin; HLA-B27, Human Leukocyte Antigen B27; HSP90AA1, Heat shock protein 90 alpha family class A member 1; IGEs, intersection genes; HPLC, High-Performance Liquid Chromatography; IL-17, Interleukin-17; IL-2, Interleukin-2; IL-4, Interleukin-4; IL-6, Interleukin-6; IL1β, Interleukin-1 beta; IBD, inflammatory bowel disease; IFN-γ, Interferon-gamma; IMQ, Imiquimod; IPA, Isopropanol; JUN, Proto-Oncogene c-Jun; KEGG, Kyoto Encyclopedia of Genes and Genomes; LC-MS/MS analysis, Liquid Chromatography-Tandem Mass Spectrometry Analysis; LEfSe, Linear Discriminant Analysis Effect Size; mzmed, The median M/Z ratio, which represents the M/Z ratio at this peak in all samples; NC, Proliferating Cell Nuclear Antigen; PASI, Psoriasis Area and Severity Index; PBS, Phosphate Buffered Saline; PCNA, Proliferating Cell Nuclear Antigen; PCA, Principal Component Analysis; PCoA, Principal Coordinates Analysis; PCR, Polymerase Chain Reaction; PDB, Protein Data Bank; PPI, Protein–Protein Interaction; PsA, psoriatic arthritis; SCFAs, short-chain fatty acids; STAT1, Signal Transducer and Activator of Transcription 1; TCM, Traditional Chinese Medicine; TCMSP, Traditional Chinese Medicine Systems Pharmacology Database; Treg, Regulatory T cells; TNF, Tumor Necrosis Factor; TGFβ1, Transforming Growth Factorβ1; UHPLC-OE-MS, Ultra-High Performance Liquid Chromatography - Orbitrap Exploris - Mass Spectrometry; rtmed, median retention time, which represents the retention time of this peak across all samples.

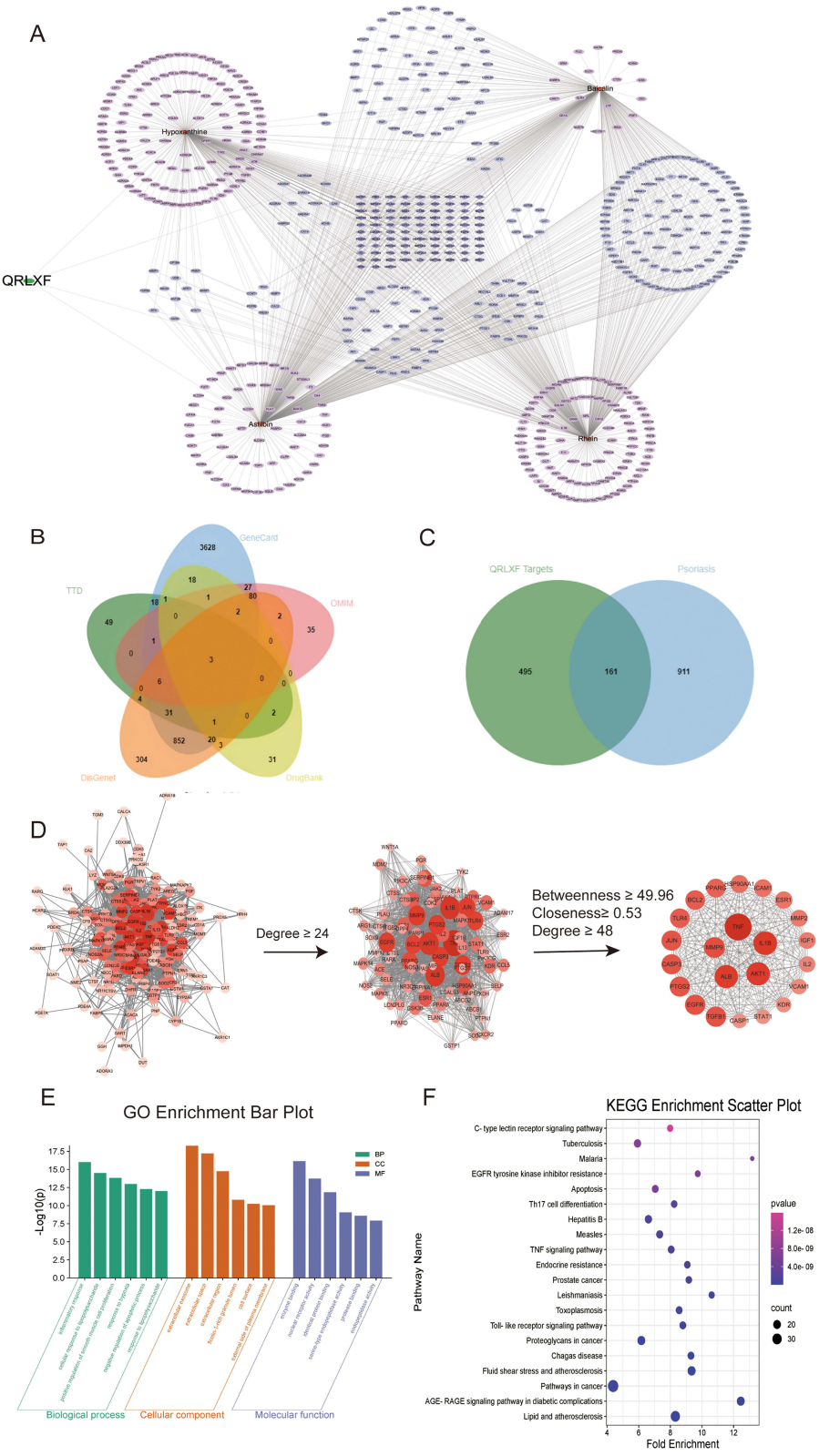

Figure 2 Potential targets and signaling pathways of QRLXF treating psoriasis predicted by network pharmacology. (**A**) Drug-component-target network diagram of QRLXF; (**B**) Psoriasis-related disease targets retrieved from databases such as TTD, OMIM, GeneCards, DisGenet, and DrugBank; (**C**) Venn diagram of the targets related to the constituents of QRLXF and those related to psoriasis; (**D**) The procedure of constructing a protein-protein interaction (PPI) network. In this network, the size and color of each node represent its degree, with a darker red color indicating a higher node degree; (**E**) GO enrichment analysis and (**F**) KEGG enrichment analysis bubble chart of the potential targets for treating psoriasis by QRLXF.

https://doi.org/10.2147/DDDT.S492044

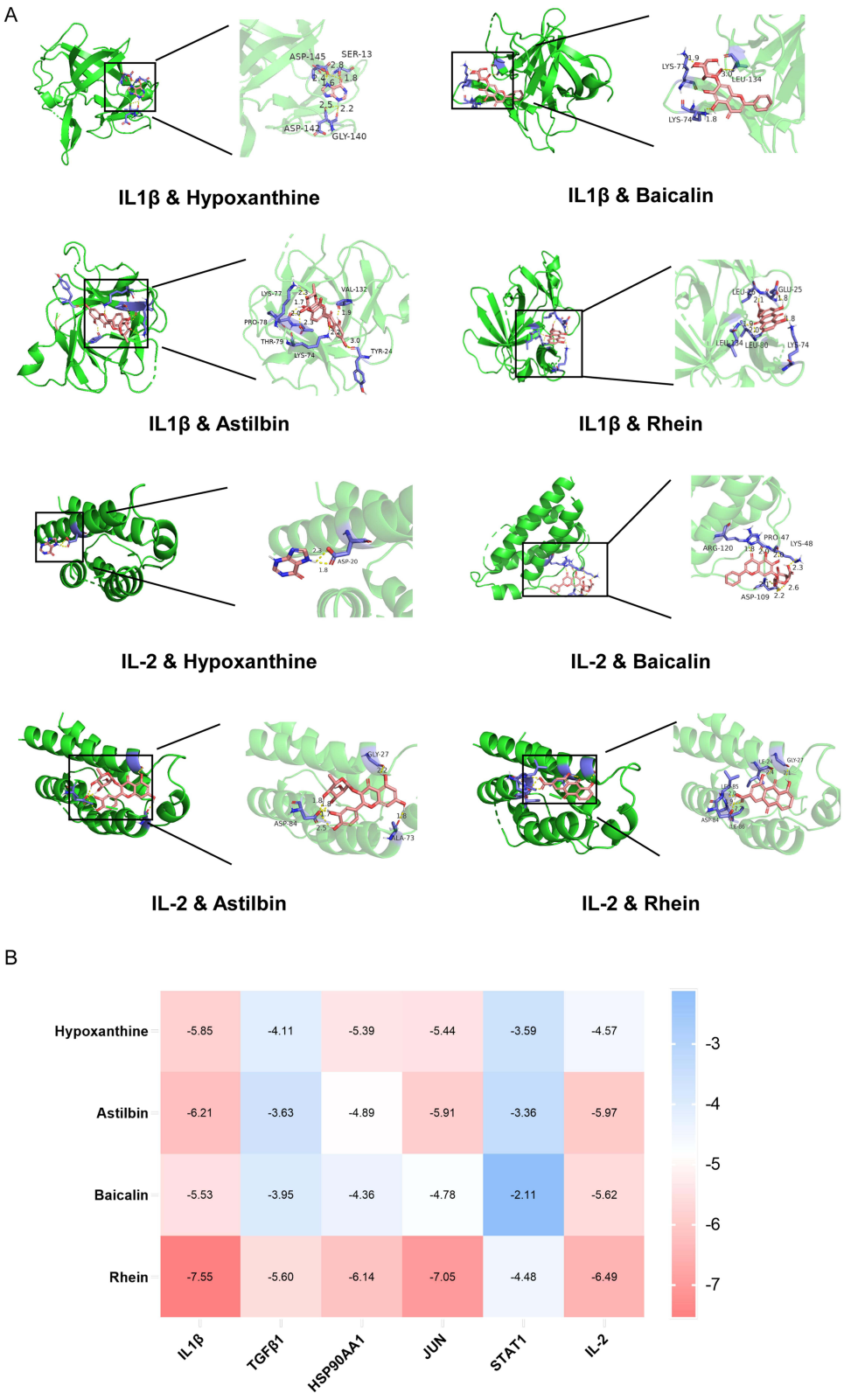

Figure 3 Molecular docking and visualization. (**A**) Molecular docking visualization using IL1β and IL-2 as examples, in which pink represents compounds, green represents target proteins, purple represents residues, yellow represents hydrogen bonds, and bond lengths are represented by numbers; (**B**) Binding energy heat map, red indicates strong binding activity, white indicates moderate binding activity, and blue indicates weak binding activity.

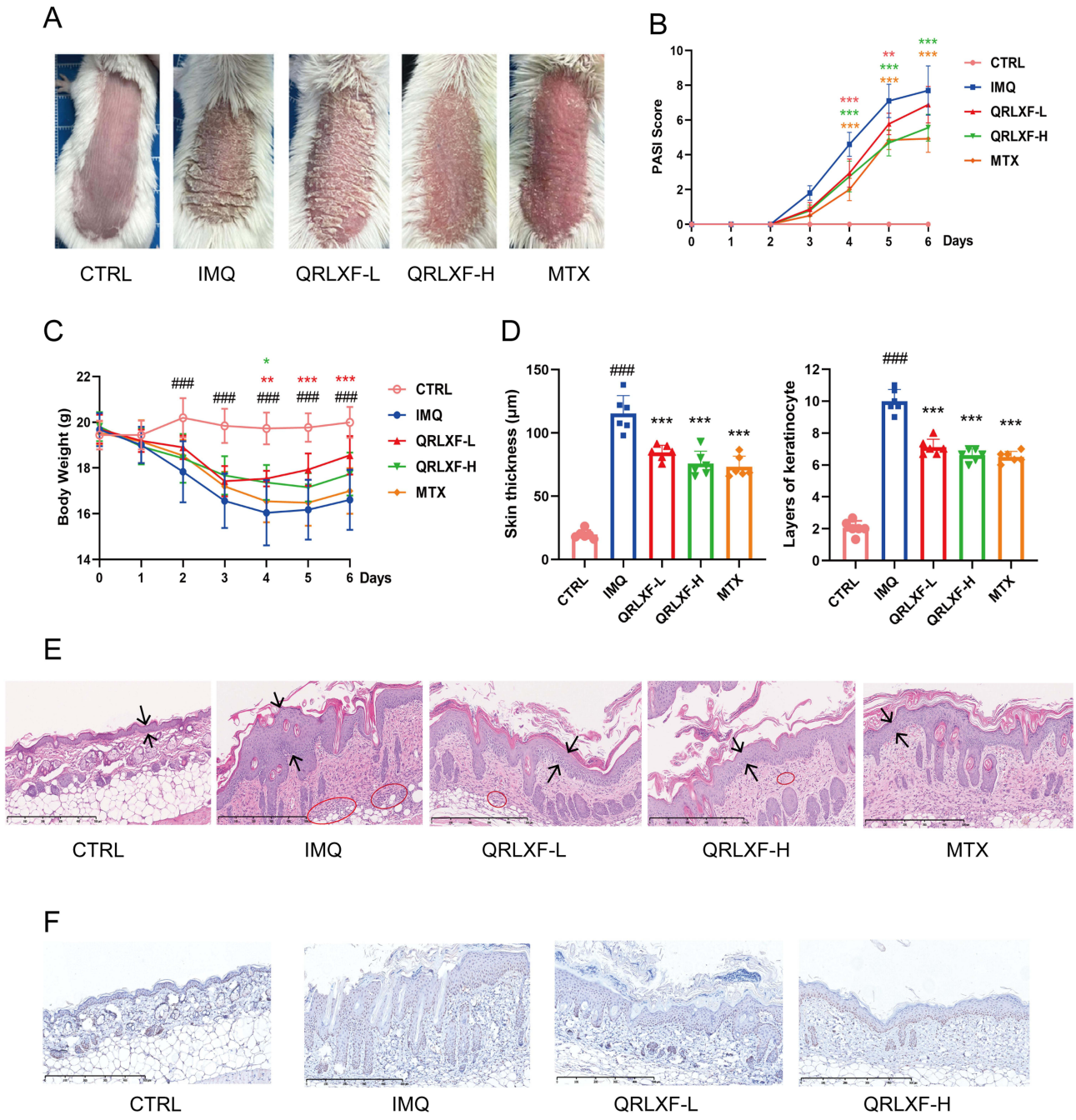

Figure 4 QRLXF ameliorated psoriasis-like skin lesions in IMQ-induced mice. (**A**) Phenotype of the back skin of mice after 6 days of topical application of IMQ; (**B**) Curve of the PASI score for back dermatitis (erythema, grading, and sclerosis); (**C**) Curves of body weight changes in mice; (**D**) skin tissue, including skin thickness and epidermal cell layers; (**E**) Schematic diagram of HE-stained scanning images of skin lesions in each group; (**F**) PCNA staining scanning images of skin lesions in each group. Unless otherwise denoted, n = 6 mice per group.

Notes: ###P < 0.001 vs CTRL; *P < 0.05, **P < 0.01, and ***P < 0.001 vs IMQ.

treatment ameliorated the skin phenotype and led to a considerable decrease in the PASI score (Figure 4B). Changes in body weight also indicate the degree of systemic inflammation. QRLXF mitigated weight loss in mice following continuous IMQ application compared to that in the IMQ group (Figure 4C).

To further evaluate inflammatory infiltration, we performed histopathological analysis of the skin lesions (Figure 4E). The results demonstrated that QRLXF markedly reduced epidermal thickness and inflammatory cell infiltration (Figure 4D). Additionally, immunohistochemical analysis revealed that QRLXF significantly decreased the number of PCNA-positive keratinocytes compared to the IMQ group (Figure 4F).

https://doi.org/10.2147/DDDT.S492044

QRLXF Can Mitigate the Inflammatory Response in Skin Lesions and Lower the Levels of Inflammatory Cytokines in Mice

Activated T cells are essential contributors to the development of psoriasis, as they initiate the release of inflammatory mediators that exacerbate inflammatory reactions in the skin. We measured the expression of these inflammatory factors in skin lesions and serum. As depicted in Figure 5A, QRLXF demonstrated a significant reduction in serum levels of IL-17A, IL-2, IL-4, TNF, and IFN-γ compared to the IMQ group. Concurrently, the levels of IL-17A, IL-2, IL-4, TNF, and IL-6 in the skin lesions of mice were markedly reduced following QRLXF treatment (Figure 5B).

QRLXF Inhibits the Differentiation of Th1/ Th17 Cells in Peripheral Immune Organs of IMQ-Induced Mice

IMQ induces inflammation both locally and systemically in mice, leading to alterations in the proportions of T lymphocytes within peripheral immune organs. The spleen index was used as a brief indicator of the immune status of the spleen. The IMQ group exhibited a notable increase in the spleen size and spleen index, whereas these parameters were notably reduced following QRLXF treatment (Figure 6A and B). The development and progression of psoriasis are driven by immune pathways mediated by Th1 and Th17 cells. T-bet and RORγT are specific transcription factors in Th1 and Th17 cells. Therefore, we evaluated the expression of these transcription factors within the CD45+CD4+ cell population of the skin-draining lymph nodes and spleens. Flow cytometry results indicated that the ratios of CD45+CD4+ T-bet+ Th1 cells and CD45+CD4+ RORγ T+ Th17 cells were obviously higher in the IMQ group than the CTRL group. This ratio was markedly reduced in the QRLXF group compared to that in the IMQ group (Figure 6C–F). This finding was also observed in the skin-draining lymph nodes and the spleen.

QRLXF Alters the Composition of Gut Microbiota in IMQ-Induced Mice

The psoriasis-like mouse model exhibited not only abnormalities in skin lesions and the immune system, but also disruptions in the intestinal microbiota. Our study found that oral QRLXF treatment reshaped the intestinal microbiota composition in IMQ-induced mice. In this study, 15 intestinal content samples were analyzed to evaluate the anti-psoriasis effects of QRLXF in IMQ-induced mice. Initially, the V3 and V4 regions of the 16SrDNA in all samples were analyzed. The rarefaction curves indicated an exceptionally high coverage across all samples. (Figure 7A). Based on the results from principal component analysis (PCA) and principal coordinate analysis (PCoA), we observed a marked distinction in the distribution of microflora among the CTRL, IMQ, and QRLXF groups (Figure 7B and D). Furthermore, we calculated the α-diversity using the Shannon and Simpson indices to assess the richness and structural variations in gut microbiota among the three groups. Our results showed that, compared to the other two groups, the model group exhibited increased gut microbiota diversity. However, as shown by the Shannon and Simpson indices, there were no significant differences in α-diversity between the CTRL and QRLXF groups (Figure 7C).

We further investigated the specific classification of the gut microbiota influenced by QRLXF. The taxonomic distribution analysis revealed variations in microbial composition across the different mouse groups. At the phylum level (Figure 7E), the phyla *Firmicutes, Proteobacteria*, and *Patescibacteria* were increased in the QRLXF group, whereas *Bacteroidetes* and *Desulfobacteria* decreased compared to those in the IMQ group. Across all the samples, *Bacteroides* and *Firmicutes* were the predominant taxa in the gut microbiota. The ratio of *Firmicutes* to *Bacteroides* (Firmicutes/Bacteroides) is a critical indicator of intestinal microbial equilibrium. At the phylum level (Figure 7E), the microbial composition of the QRLXF group was similar to that of the CTRL group. Moreover, Firmicutes/Bacteroides in the QRLXF group was higher than that in the IMQ group (Figure 7F). The levels of the genera *Ligilactobacillus, Lactobacillus*, and *Candidatus saccharimon* in the QRLXF group were increased, whereas that of *Enterorhabdus, Helicobacter*, and *Anaerotruncus* were reduced compared with the IMQ group (Figure 7G). The heat maps further showed that the abundance of *Lactobacillus* and *Candidatus saccharimon* was significantly higher in the CTRL group than in the other two groups. QRLXF treatment significantly increased the abundance of *Ligilactobacilli*. Additionally, Firmicutes comprised most of the dominant microbiota in both the CTRL and QRLXF groups (Figure 7H).

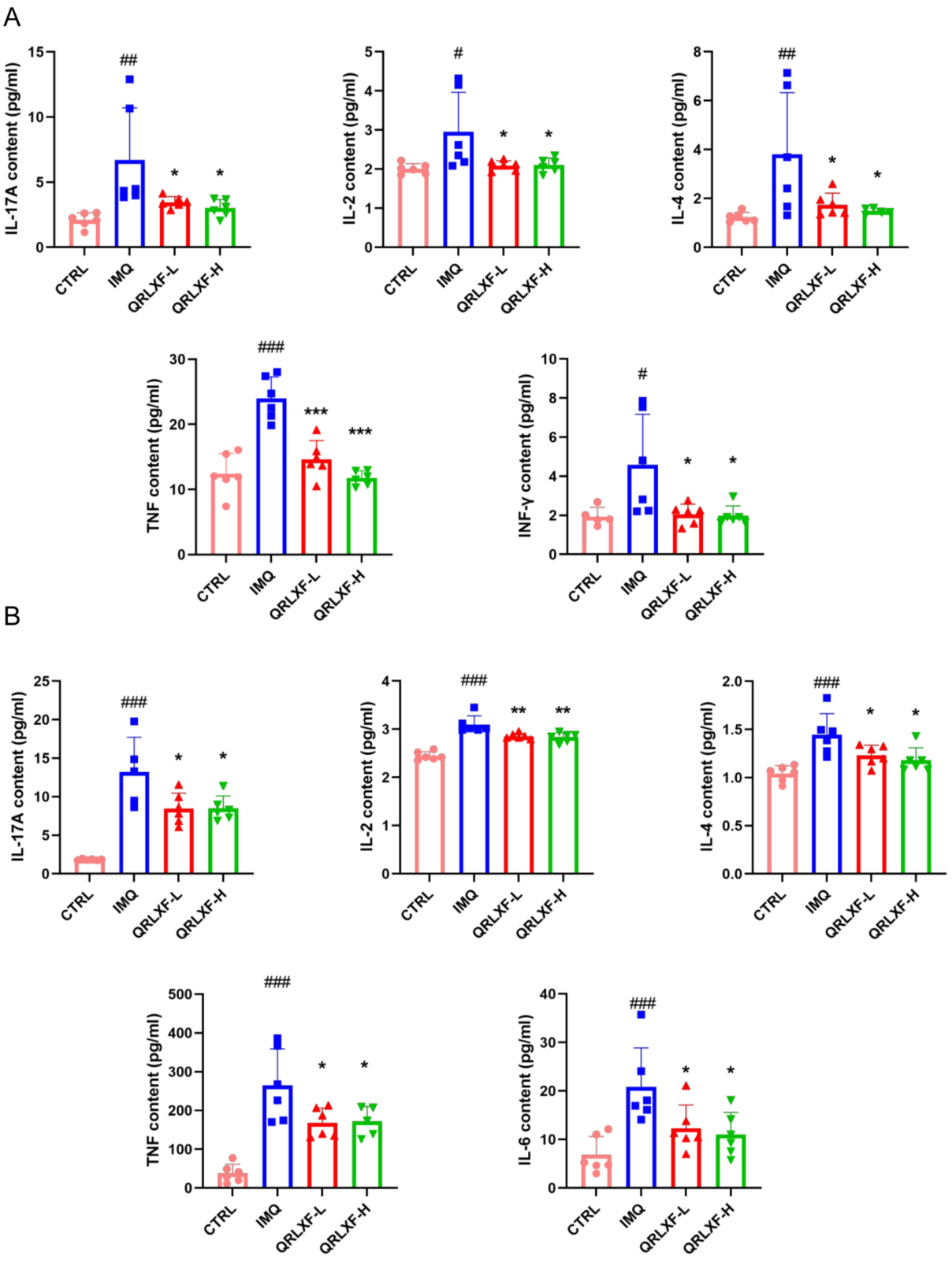

Figure 5 QRLXF reduced the release of inflammatory factors in IMQ-induced mice. (**A**) The content of IL-17A, IL-2, IL-4,TNF and INF-γ in serum; (**B**) The content of IL-17A, IL-2, IL-4,TNF and IL-6 in skin lesions; Unless otherwise denoted, n = 6 mice per group.
Notes: $^{\#}P < 0.05$, $^{\#\#}P < 0.01$, and $^{\#\#\#}P < 0.001$ versus CTRL; $^{*}P < 0.05$, $^{**}P < 0.01$, and $^{***}P < 0.001$ versus IMQ.

https://doi.org/10.2147/DDDT.S492044

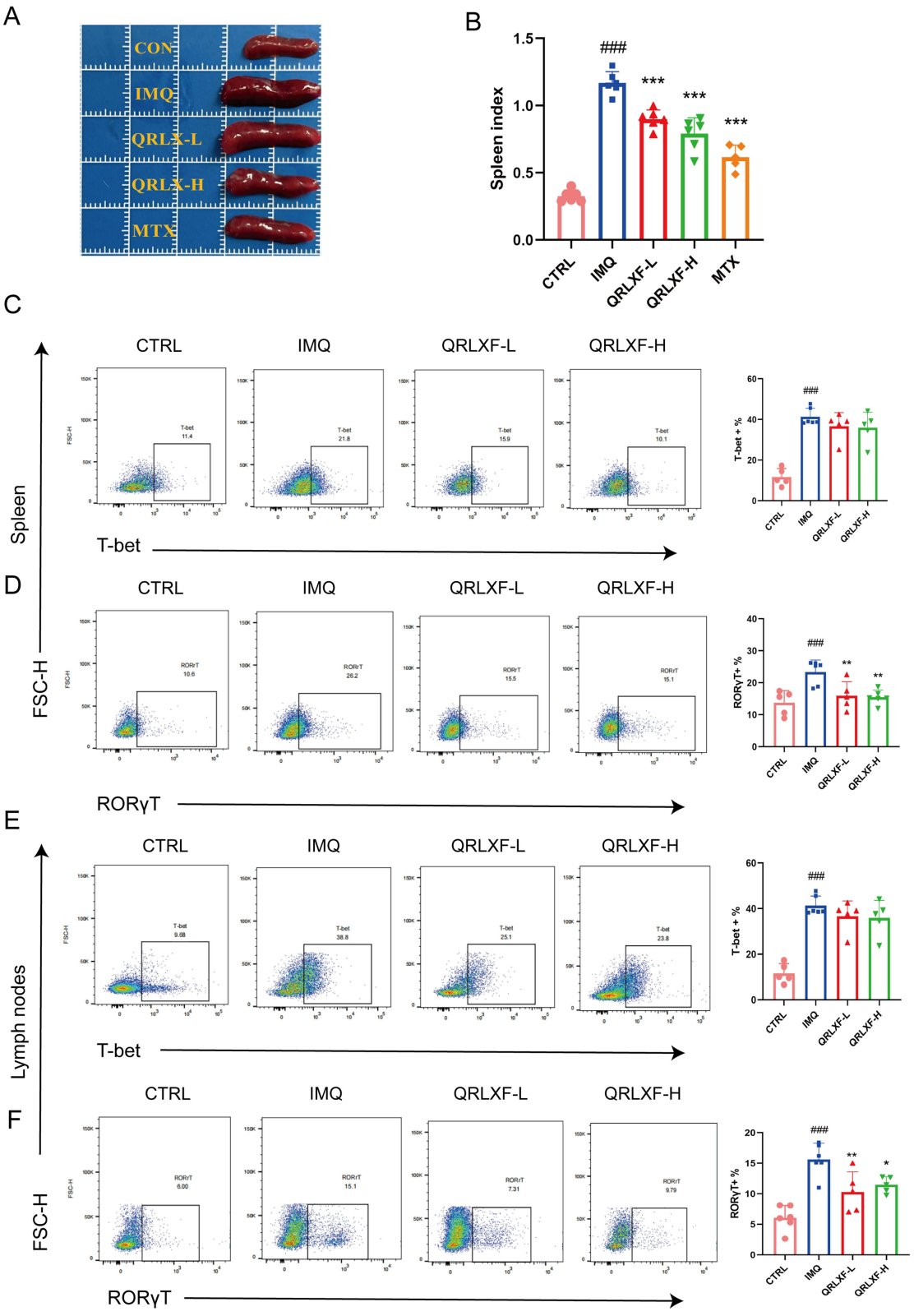

Figure 6 QRLXF regulates the differentiation of CD4+T cells in psoriasis-like mice. (**A**) The morphological observation of the spleen in each group; (**B**) Spleen indexes in each group; Spleen indexes are expressed by the specific organ index [(organ weight/body weight)*100]; (**C**) Flow cytometric gating strategy and proportion of Th1 cells (CD45+CD4+T-bet+) in the spleen (**D**) Flow cytometric gating strategy and proportion of Th17 cells (CD45+CD4+ RORγT +) in spleens; (**E**) Flow cytometric gating strategy and proportion of Th1 cells (CD45+CD4+T-bet+) in lymph nodes; (**F**) Flow cytometric gating strategy and proportion of Th17 cells (CD45+CD4+ RORγT +) in lymph nodes. Unless otherwise denoted, n = 5–6 mice per group.

Notes: $^{###}P < 0.001$ versus CTRL; $^{*}P < 0.05$, $^{**}P < 0.01$, and $^{***}P < 0.001$ versus IMQ.

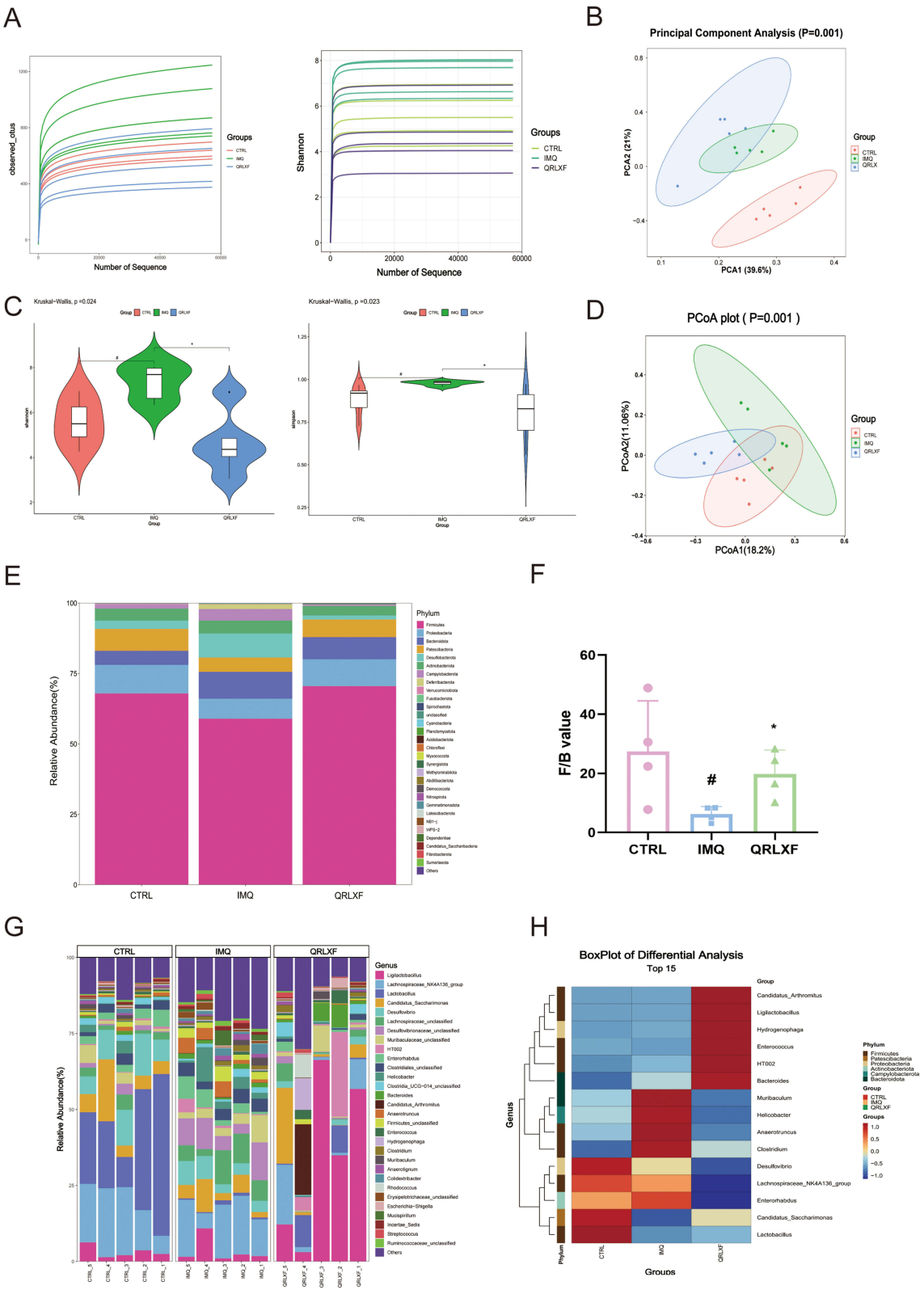

Figure 7 Effects of QRLXF on the composition of gut microbiota in IMQ-induced mice. (**A**) Species accumulation curves had reached a plateau; (**B**) PCA and (**D**) PCoA plots of β-diversity; (**C**) α-diversity analysis based on the Shannon index and Simpson index; (**E**) The relative abundance (%) of the intestinal microbiota was determined at the phylum level; (**F**) Firmicutes/Bacteroides value; (**G**) The relative abundance (%) of the intestinal microbiota was determined at the genus level; (**H**) Heat map of microbiota composition at the phylum and genus level; n = 5 mice per group.

Notes: $^{\#}P < 0.05$ versus CTRL; $^{*}P < 0.05$ versus IMQ.

https://doi.org/10.2147/DDDT.S492044

QRLXF Affects the Abundance of Specific Flora and Alters the Biological Function of the Gut Microbiota in IMQ-Induced Mice

To identify potential biomarkers critical for psoriasis treatment, we conducted a differential analysis. Using the Kruskal–Wallis *H*-test, we evaluated the differences in the composition of the gut microbiota across the three groups (Figure 8A and B). The results showed that 17 microbes at genus level differed significantly among the three groups. These microbial genera included *Ligilactobacillus, Lactobacillus, A2, Anaerotruncus, Bilophila, Colidextribacter, Eisenbergiella, Eubacterium,*

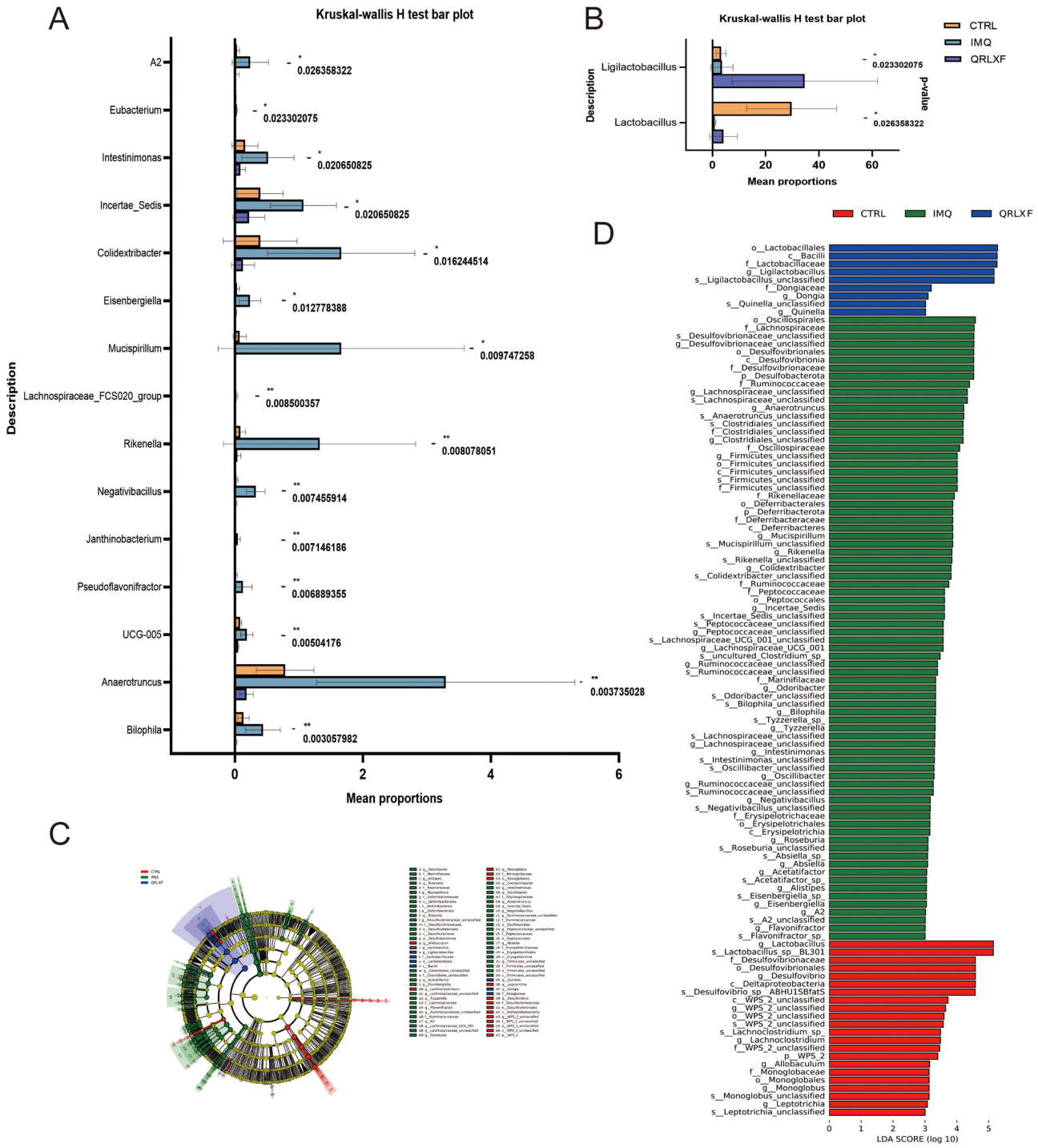

Figure 8 Continued.

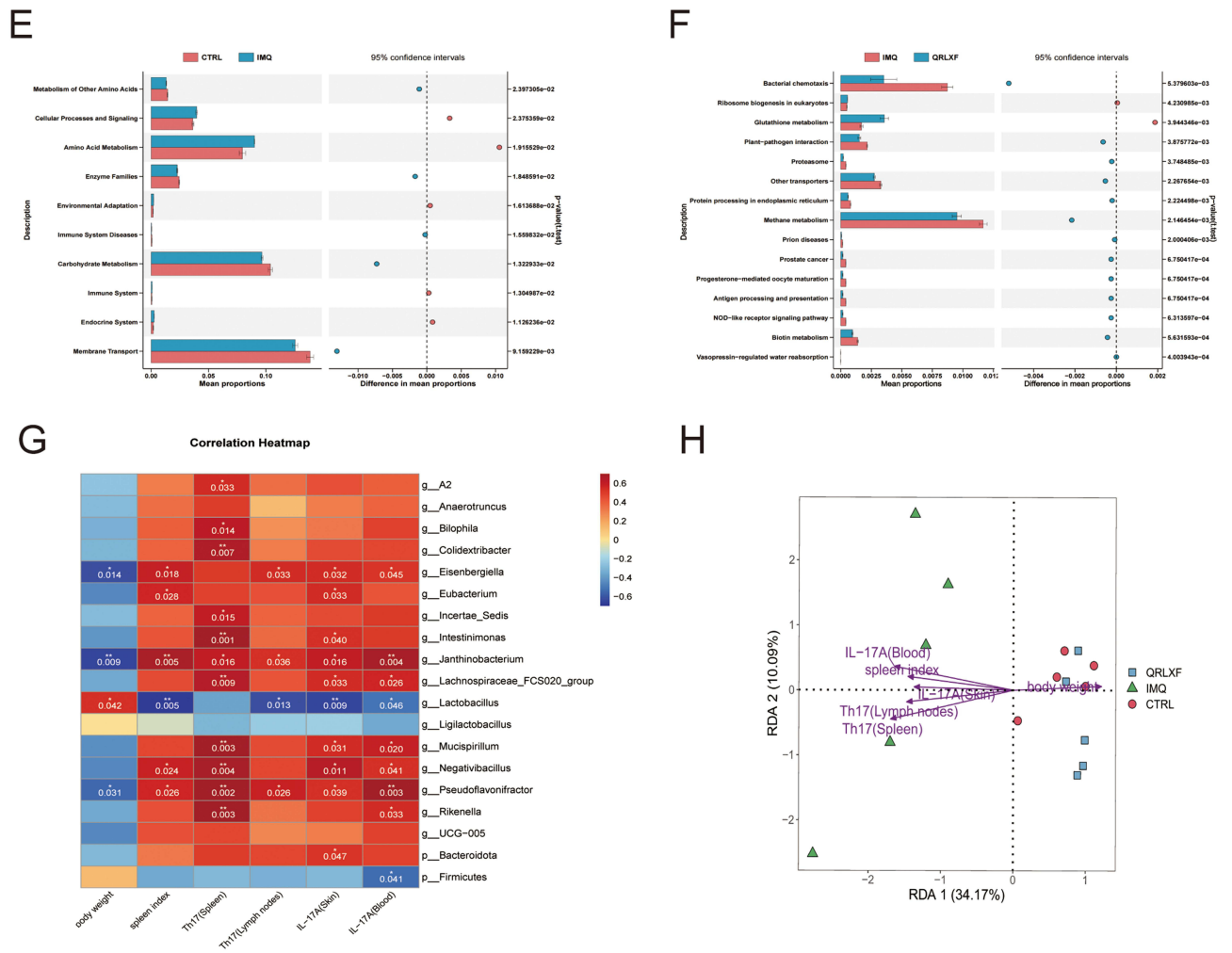

Figure 8 Potential biomarkers of QRLXF therapy and its effect on fecal biological function of IMQ-induced mice. (**A** and **B**) Relative abundance of the significantly altered bacteria at the genus level across the three groups. Data are presented as the mean± sem. n = 5. * P < 0.05; ** P < 0.01; (**C**) Cladogram and (**D**) histogram of LEfSe comparison of gut microbiota among CTRL, IMQ, and QRLXF groups (LDA score > 3.0, P <0.05); (**E**) Comparison of KEGG pathways between the CTRL group and the IMQ group; (**F**) Functional differences in KEGG pathways between the IMQ group and the QRLXF group; (**G**) Correlation analysis of differential genera and psoriasis-related factors. The colors ranged from red (positive correlation) to blue (negative correlation). *P < 0.05, and **P < 0.01; (**H**) RDA analysis. Each point in the diagram represents a sample, and the closer the distance between the two points, the more similar the community structure of the two samples. The arrows represent different influencing factors, respectively. When the angle between the influencing factors (between the factor and the sample) is acute, the two factors are positively correlated, and when the angle is obtuse, the two factors are negatively correlated. The longer the ray, the greater the role of the factor.

Incertae_Sedis, Intestinimonas, Janthinobacterium, Lachnospiraceae_FCS020_group, Mucispirillum, Negativibacillus, Pseudoflavonifractor, Rikenella, and *UCG-005*. QRLXF treatment increased the abundance of the genera *Ligilactobacillus* and *Lactobacillus*. Additionally, it corrected the gut microbiota imbalance caused by IMQ treatment by significantly reducing the abundance of the other 15 genera.

We also employed LEfSe analysis at the genus level to identify the bacterial taxa that differed significantly among the three groups. The genera *Ligilactobacillus, Dongia*, and *Quinella* were notably enriched in the QRLXF group. In contrast, the IMQ group showed notable enrichment of genera such as *Bilophila, Anaerotruncus, Negativibacillus, Mucispirillum*, and *Eisenbergiella* (Figure 8C and D).

To gain a better understanding of the potential impact of QRLXF therapy on biological processes, we used PICRUSt2 to assess the functional gene composition of the gut microbiota in our samples. Subsequent analyses were performed using the KEGG database. In the IMQ group, there was a notable enrichment of functional genes related to the immune system, environmental adaptation, amino acid metabolism, and cellular processes, whereas genes associated with carbohydrate metabolism and enzyme families were reduced compared to those in the CTRL group (Figure 8E).

https://doi.org/10.2147/DDDT.S492044

Functional genes involved in carbohydrate metabolism were significantly enriched in the QRLXF group, whereas genes involved in the immune system, amino acid metabolism, cellular processes and signaling, cell motility, and environmental adaptation were reduced compared to those in the IMQ group (Figure 8F).

According to recent studies, the gut is an important immunological organ, and the gut microbiota play an essential role in the formation of the intestinal microenvironment. Changes in the composition and abundance of microbial communities can substantially affect the immune status within the gut and systemically throughout the body. We identified 17 distinct genera of bacteria and conducted a correlation analysis with psoriasis-related factors to investigate the relationship between QRLXF-induced alterations in the gut microbiota and Th17-related immune responses. Correlation analysis was performed to investigate the relationships between body weight, spleen index, Th17 cell ratio, levels of IL-17A levels, and specific bacterial genera. Correlation heat maps (Figure 8G) revealed that the abundance of multiple genera enriched in IMQ-induced mice was positively correlated with the proportion of Th17 cells and IL-17A levels, including *Eisenbergiella, Janthinobacterium, Lachnospiraceae_FCS020_group, Mucispirillum, Negativibacillus*, and *Pseudoflavonifractor*. Notably, significant negative correlations were observed between the abundance of Lactobacillus and the spleen index, proportion of Th17 cells in lymph nodes, and levels of IL-17A in both skin lesions and serum.

RDA demonstrated a correlation between psoriasis-related factors and intestinal microbiota across the three groups. As depicted in Figure 8H, the arrows represent the proportion of Th17 cells in the spleen and lymph nodes as well as the levels of IL-17A in skin lesions and serum, all pointing toward the samples of the IMQ group, indicating that the increase in the Th17-related inflammatory response is positively correlated with the changes in the species community in the IMQ group.

Discussion

Psoriasis is an immune-mediated, inflammatory, and systemic disease caused by the interactions between genetic and environmental factors. Owing to its chronic and relapsing nature, psoriasis poses a significant therapeutic challenge and often results in lifelong suffering for patients. Traditional Chinese Medicine (TCM) has a profound historical background on the understanding and treatment of psoriasis. Qingreliangxuefang (QRLXF), composed of 11 ingredients from Traditional Chinese Medicine, is effective in clearing heat, detoxifying, eliminating dampness, nourishing Yin, and enhancing blood circulation. In clinical practice, QRLXF has demonstrated notable efficacy in treatment of psoriasis. However, owing to the intricate nature of its composition and structure, its mechanism of action has not yet been thoroughly examined.

This study employed LC-MS/MS analysis along with systemic pharmacology analysis to preliminarily identify the active ingredients in QRLXF and analysed its potential targets. By integrating this information with the signalling pathways associated with these targets, we predicted the potential mechanism of action of QRLXF. Subsequently, we investigated the mechanism by which QRLXF alleviated IMQ-induced skin damage. QRLXF treatment significantly alleviated psoriasis-like symptoms in IMQ-induced mice. Furthermore, the expression of various T cell subtypes, including Th1 and Th17, in the immune organs of IMQ-induced mice was found to be modulated by QRLXF, and the levels of cytokines mediating Th17 differentiation in skin lesions and serum decreased after treatment. Simultaneously, oral administration of QRLXF regulated the disrupted intestinal flora in IMQ-induced mice. After treatment with QRLXF, mice exhibited a microbiota profile with increased proportions of *Ligilactobacillus* and *Lactobacillus*, whereas the genera *Anaerotruncus, Negativibacillus, Mucispirillum*, and *Bilophila* were decreased. These findings suggest that QRLXF may suppress the onset of an inflammatory cytokine storm and adjust the intestinal flora composition in a psoriatic mouse model, potentially modulating the inflammatory response in psoriasis.

Recently, the role of the gut as an immunological organ has received increasing attention. The intestines contain a significant portion of the body's lymphoid tissue. T lymphocytes in the intestinal epithelium and lamina propria exhibit effector phenotypes, which are thought to contribute to maintaining the balance between the luminal commensal microflora and intestinal histiocytes.[21] Th17 cells are abundant in both the skin and gut, with the latter being a critical site for regulating their proliferation and differentiation.[41,42] The development and accumulation of Th17 cells in the gastrointestinal tract depend on the response to colonisation by certain gut microbiota and extracellular pathogens.[43] It is widely acknowledged that animals in germ-free environments often have underdeveloped immune systems. A significant

reduction in CD4+ T cells was noted in the lamina propria of germ-free mouse intestines, whereas colonisation with intestinal microflora led to rapid expansion and differentiation of effector and regulatory T cells. RORγt+Foxp3-Th17 cells and Foxp3+ regulatory T (Treg) cells are among the most prominently induced cells.[44–46] Thus, the composition of intestinal bacteria plays a critical role in the differentiation of Th17 cells and their balance with Treg cells within the intestinal lamina propria. Moreover, the immune dysfunction induced by microorganisms can extend beyond the gut and potentially trigger systemic immune responses. This phenomenon is closely linked to an individual's genetic predisposition.[47] For instance, Bacteroides fragilis in the intestine influences the systemic Th1 response via its derived polysaccharide A (PSA).[48] Thus, alterations in gut microbiota are hypothesized to affect an individual's susceptibility to autoimmune diseases,[49] inflammatory disorders,[50] and infections in both intestinal and distant tissues,[49,51,52] and possibly contribute to systemic immune-inflammatory conditions.[53,54]

Studies have suggested a link between disturbances in gut microbiota composition and the development of psoriasis. This appears to be intimately connected to immune responses mediated by Th17 cells. Subclinical histological and molecular signs of intestinal inflammation have been observed in patients with psoriasis without bowel disease symptoms along with an increase in intestinal lamina propria cells.[55] This suggests a pathogenic link between cutaneous lesions and the gut in these patients. Animal models provide additional evidence supporting the role of the gut microbiota in the onset of psoriasis. Following antibiotic administration, IMQ-induced mice exhibited a diminished level of both local and systemic Th17 cell activation, along with decreased severity of psoriasis-like skin inflammation.[30] It is suggested that changes in the gut flora might regulate IMQ-induced skin inflammation by modulating the Th17 cell response.

Firmicutes and Bacteroidetes are the dominant phyla in the gut microbiota. Maintaining a balance between Firmicutes and Bacteroidetes is essential for sustaining homeostasis, and disruptions in this ratio have been associated with the onset of various pathologies.[56] Maintaining this balance is crucial for modulating intestinal inflammation and preserving the integrity of the intestinal barrier.[57,58] Our findings suggest that QRLXF therapy is associated with an increased F/B ratio, which predicts higher butyrate production.[59,60] Butyrate, a short-chain fatty acid (SCFA), can reduce oxidative stress in the colonic mucosa and regulate the Th17/Treg lymphocyte balance, thus protecting the intestinal epithelium from exposure to toxins and pathogenic microorganisms.[61,62] Additionally, treatment with secukinumab, an IL-17 inhibitor, regulates the gut microbiome and elevates the F/B ratio in psoriatic patients, potentially modulating gut dysbiosis through metabolic pathways and providing significant anti-inflammatory effects.[63]

The progression from localised microenvironmental disturbances to systemic immune dysfunction in psoriasis may be due to a weakened intestinal mucosal barrier.[64] Damage to the epithelial cell surface may compromise both physical and immunological barriers, allowing certain microorganisms to promote disease.[65,66] Studies have demonstrated that erosion of the gut lining might engender vulnerability to autoimmune and inflammatory disorders by exposing bacterial antigens to the host's immune system.[67] Bacterial DNA has been found in the circulatory system of some individuals with psoriasis. Moreover, serum levels of inflammatory cytokines were higher in these individuals than in those without bacterial DNA. These individuals also tended to have a longer disease course and earlier onset.[53] This suggests a possible link between worsening psoriasis and intestinal bacterial translocation. Biomarkers of intestinal permeability, such as elevated claudin-3 and intestinal fatty acid-binding protein levels, have been identified the sera of patients with psoriasis.[68] These findings confirm the impaired function of the intestinal mucosal barrier in psoriasis patients.

Our study revealed a reduction in the deleterious bacteria associated with intestinal inflammation and impaired barrier function after QRLXF therapy. *Negativibacillus*, a harmful bacterium, significantly increases in patients with ulcerative colitis.[69] Its abundance is positively correlated with diamine oxidase (DAO) levels, a marker of intestinal damage.[70] *Anaerotruncus* is linked to a higher risk of colorectal cancer.[71] Its accumulation leads to the dysregulation of the gut microbiota and compromised intestinal barrier integrity, disrupting amino acid metabolism and amplifying inflammation mediated by CD4+ Th17 cells.[72] *Mucispirillum*, a pathogenic bacterium, is widespread throughout the digestive tract. Its flagella enable it to cross the mucosal barrier, causing intestinal inflammation.[73,74] *Anaerotruncus* and *Mucispirillum* are linked to psoriasis-related comorbidities, potentially increasing intestinal permeability and endotoxin levels in the bloodstream. This process, associated with metabolic syndrome, may lead to systemic inflammation and oxidative stress.[75–78] *Bilophila* can increase the susceptibility to inflammatory disorders and trigger an exaggerated immune response in both mucosal and systemic conditions, particularly against a background of mild systemic inflammation.[79,80]

There has been an increasing interest in disease prevention and treatment via manipulation of the intestinal microenvironment. This approach has demonstrated encouraging results in the treatment of psoriasis. Researchers have found that oral probiotic treatment positively affects disease progression in patients with psoriatic arthritis (PsA). Moreover, the levels of intestinal permeability markers were found to correlate with the prevalence of peripheral Th17 cells.[81] In our study, we found that the QRLXF group had a significantly higher proportion of Lactobacillus species at the genus level than the IMQ-induced mice. Correlational analysis further indicated that psoriatic inflammatory indices, including the Th17 cell ratio in immune tissues and pro-inflammatory cytokines in skin plaques, were negatively associated with *Lactobacillus* abundance. *Lactobacillus* can restore gut barrier integrity by strengthening intestinal epithelial tight junctions and reducing intestinal inflammation via the secretion of short-chain fatty acids (SCFAs).[82,83] Oral administration of *L. pentosus GMNL-77* significantly reduced erythematous scaling lesions in IMQ-induced mice, and decreased the population of IL-17-secreting CD4+ T cells in the spleen.[84] *Lactobacillus* has also been used in clinical treatment. The oral intake of *Lactobacillus casei* can alleviate antigen-specific skin inflammation.[85,86] *Ligilactobacillus* is another common probiotic that can protect the colorectal barrier by lowering serum inflammatory cytokine levels and preventing bacterial translocation.[87,88] Research has shown that *Lactobacillus* and *Ligilactobacillus* notably reduce intestinal inflammation in murine models and play a key role in the transition from acute to chronic colitis.[89]

The present study found that QRLXF treatment increased the number of probiotics and decreased the number of potentially pathogenic microbes in the intestinal flora. These changes reduced intestinal immune-mediated inflammation and strengthened the intestinal barrier. Furthermore, QRLXF balances the immune response of T lymphocytes, especially Th17 cells.

However, our study has several limitations. To obtain more comprehensive and reliable results, we suggest the following research endeavours: metagenomic analyses should be conducted to clarify the functional roles of gut microbiota. Additionally, bioactivity assessments and faecal transplant trials should focus on specific intestinal microbiota. Subsequently, expanding the sample size and integrating the clinical data will facilitate further investigation. Finally, identifying the effective components and optimal dosage of QRLXF for treating psoriasis-affected mice with disrupted gut flora, along with pharmacological analyses, is crucial.

Conclusion

This study demonstrated that Qingreliangxuefang was effective in alleviating psoriasis-like clinical symptoms in IMQ-treated mice. In addition, it reshapes the gut microbiome and modulates the Th17 cell response. It is worth noting that oral administration of Qingreliangxuefang significantly increased the abundance of two crucial probiotic strains in the gut while suppressing certain pathogens linked to intestinal inflammation and metabolic dysfunction. These probiotics may exert therapeutic effects on psoriasis by inhibiting Th17-cell-associated inflammation. This investigation represents a hopeful stride in exploring the effects of herbal formulations on psoriasis.In the future, the effective dose of QRLXF can be further optimized, and clinical trials can be conducted to evaluate its safety and efficacy in human patients.

Acknowledgments

We would like to acknowledge the support of bioinformatics and FigDraw for the graphical representations in this study and LC-BIO TECHNOLOGIES (HANGZHOU) CO, LTD for the technical support. Also, We thank the National Clinical Research Center for Skin and Immune Diseases, Beijing, China, for their support of this study.

Funding

This study was sponsored by the Zhejiang Key Laboratory of Dermatology of Integrated Traditional Chinese and Western Medicine [Project No. 2A11829 (Finance 201808) L.L.M], Zhejiang Provincial Famous Traditional Chinese Medicine Practitioner Ma Lili's Studio [Project No. 1×12204 (Finance 20220801) L.L.M], the National Natural Science Foundation of China (Grant 82274175 and 82474168 to Q.Y.S. Grant 82174026 to H.Y.F.), the Natural Science Foundation of Zhejiang Province (Grant LY22H280012 to H.Y.F.), the Key Project of Natural Science Foundation of Zhejiang Province (No. LZ20H290001), Zhejiang Provincial Administration of Traditional Chinese Medicine Co-construction Key Project (Grant GZY-ZJ-KJ-23069 to Q.Y.S.), Zhejiang Provincial Program for the Cultivation of

High-level Innovative Health talent, Zhejiang Province Traditional Chinese medicine science and technology project (Grant 2024ZL1157 to Y.F.L, Grant 2019ZQ024 to Y.M.F).

Disclosure

The authors state that the study was done without any commercial or financial links that may be seen as a possible conflict of interest.

References

1. Griffiths CE, Barker JN. Pathogenesis and clinical features of psoriasis. *Lancet*. 2007;370(9583):263–271. doi:10.1016/S0140-6736(07)61128-3
2. Cao F, Liu Y-C, Ni Q-Y, et al. Temporal trends in the prevalence of autoimmune diseases from 1990 to 2019. *Autoimmun Rev*. 2023;22(8):103359. doi:10.1016/j.autrev.2023.103359
3. Parisi R, Iskandar IYK, Kontopantelis E, Augustin M, Griffiths CEM, Ashcroft DM. National, regional, and worldwide epidemiology of psoriasis: systematic analysis and modelling study. *BMJ*. 2020;369:m1590. doi:10.1136/bmj.m1590
4. Xiao Y, Hong X, Neelagar R, Mo H. Age-standardized incidence, prevalence, mortality rates and future projections of autoimmune diseases in China: a systematic analysis based on GBD 2021. *Immunol Res*. 2025;73(1):26. doi:10.1007/s12026-024-09591-5
5. Lebwohl M. Psoriasis. *Ann Intern Med*. 2018;168(7):ITC49–ITC64. doi:10.7326/AITC201804030
6. Langley RG, Elewski BE, Lebwohl M, et al. Secukinumab in plaque psoriasis–results of two Phase 3 trials. *N Engl J Med*. 2014;371(4):326–338. doi:10.1056/NEJMoa1314258
7. Papp KA, Langley RG, Sigurgeirsson B, et al. Efficacy and safety of secukinumab in the treatment of moderate-to-severe plaque psoriasis: a randomized, double-blind, placebo-controlled Phase II dose-ranging study. *Br J Dermatol*. 2013;168(2):412–421. doi:10.1111/bjd.12110
8. Ma X, Li T, Han G. Two cases of immune drift phenomena caused by biologic agents for treating psoriasis and atopic dermatitis. *Clin Cosmet Invest Dermatol*. 2023;16:3521–3525. doi:10.2147/CCID.S445468
9. Lebwohl MG, Bachelez H, Barker J, et al. Patient perspectives in the management of psoriasis: results from the population-based multinational assessment of psoriasis and psoriatic arthritis survey. *J Am Acad Dermatol*. 2014;70(5). doi:10.1016/j.jaad.2013.12.018
10. Guo J, Zhang H, Lin W, Lu L, Su J, Chen X. Signaling pathways and targeted therapies for psoriasis. *Signal Transduct Target Ther*. 2023;8(1):437. doi:10.1038/s41392-023-01655-6
11. van der Fits L, Mourits S, Voerman JSA, et al. Imiquimod-induced psoriasis-like skin inflammation in mice is mediated via the IL-23/IL-17 axis. *J Immunol*. 2009;182(9):5836–5845. doi:10.4049/jimmunol.0802999
12. Subudhi I, Konieczny P, Prystupa A, et al. Metabolic coordination between skin epithelium and type 17 immunity sustains chronic skin inflammation. *Immunity*. 2024;57(7):1665–1680.e7. doi:10.1016/j.immuni.2024.04.022
13. Ghoreschi K, Balato A, Enerbäck C, Sabat R. Therapeutics targeting the IL-23 and IL-17 pathway in psoriasis. *Lancet*. 2021;397(10275):754–766. doi:10.1016/S0140-6736(21)00184-7
14. Eppinga H, Sperna Weiland CJ, Thio HB, et al. Similar depletion of protective faecalibacterium prausnitzii in psoriasis and inflammatory bowel disease, but not in hidradenitis suppurativa. *J Crohns Colitis*. 2016;10(9):1067–1075. doi:10.1093/ecco-jcc/jjw070
15. Xiao S, Zhang G, Jiang C, et al. Deciphering gut microbiota dysbiosis and corresponding genetic and metabolic dysregulation in psoriasis patients using metagenomics sequencing. *Front Cell Infect Microbiol*. 2021;11:605825. doi:10.3389/fcimb.2021.605825
16. Hidalgo-Cantabrana C, Gómez J, Delgado S, et al. Gut microbiota dysbiosis in a cohort of patients with psoriasis. *Br J Dermatol*. 2019;181(6):1287–1295. doi:10.1111/bjd.17931
17. Zhang X, Shi L, Sun T, Guo K, Geng S. Dysbiosis of gut microbiota and its correlation with dysregulation of cytokines in psoriasis patients. *BMC Microbiol*. 2021;21(1):78. doi:10.1186/s12866-021-02125-1
18. Shapiro J, Cohen NA, Shalev V, Uzan A, Koren O, Maharshak N. Psoriatic patients have a distinct structural and functional fecal microbiota compared with controls. *J Dermatol*. 2019;46(7):595–603. doi:10.1111/1346-8138.14933
19. Pinget GV, Tan JK, Ni D, et al. Dysbiosis in imiquimod-induced psoriasis alters gut immunity and exacerbates colitis development. *Cell Rep*. 2022;40(7):111191. doi:10.1016/j.celrep.2022.111191
20. De Pessemier B, Grine L, Debaere M, Maes A, Paetzold B, Callewaert C. Gut-skin axis: current knowledge of the Interrelationship between microbial dysbiosis and skin conditions. *Microorganisms*. 2021;9(2). doi:10.3390/microorganisms9020353
21. Omenetti S, Bussi C, Metidji A, et al. The intestine harbors functionally distinct homeostatic tissue-resident and inflammatory Th17 cells. *Immunity*. 2019;51(1):77–89.e6. doi:10.1016/j.immuni.2019.05.004
22. Barcik W, Boutin RCT, Sokolowska M, Finlay BB. The role of lung and Gut microbiota in the pathology of asthma. *Immunity*. 2020;52(2):241–255. doi:10.1016/j.immuni.2020.01.007
23. Mahmud MR, Akter S, Tamanna SK, et al. Impact of gut microbiome on skin health: gut-skin axis observed through the lenses of therapeutics and skin diseases. *Gut Microbes*. 2022;14(1):2096995. doi:10.1080/19490976.2022.2096995
24. Rath HC, Herfarth HH, Ikeda JS, et al. Normal luminal bacteria, especially Bacteroides species, mediate chronic colitis, gastritis, and arthritis in HLA-B27/human beta2 microglobulin transgenic rats. *J Clin Invest*. 1996;98(4):945–953. doi:10.1172/JCI118878
25. Zhou B, Yuan Y, Zhang S, et al. Intestinal flora and disease mutually shape the regional immune system in the intestinal tract. *Front Immunol*. 2020;11:575. doi:10.3389/fimmu.2020.00575
26. Sun C-Y, Yang N, Zheng Z-L, Liu D, Xu Q-L. T helper 17 (Th17) cell responses to the gut microbiota in human diseases. *Biomed Pharmacother*. 2023;161:114483. doi:10.1016/j.biopha.2023.114483
27. Valiente GR, Munir A, Hart ML, et al. Gut dysbiosis is associated with acceleration of lupus nephritis. *Sci Rep*. 2022;12(1):152. doi:10.1038/s41598-021-03886-5
28. Wu H-J, Ivanov II, Darce J, et al. Gut-residing segmented filamentous bacteria drive autoimmune arthritis via T helper 17 cells. *Immunity*. 2010;32(6):815–827. doi:10.1016/j.immuni.2010.06.001

29. Jin S, Zhao D, Cai C, et al. Low-dose penicillin exposure in early life decreases Th17 and the susceptibility to DSS colitis in mice through gut microbiota modification. *Sci Rep*. 2017;7(1):43662. doi:10.1038/srep43662
30. Zákostelská Z, Málková J, Klimešová K, et al. Intestinal microbiota promotes psoriasis-like skin inflammation by enhancing Th17 response. *PLoS One*. 2016;11(7):e0159539. doi:10.1371/journal.pone.0159539
31. Stehlikova Z, Kostovcikova K, Kverka M, et al. Crucial role of microbiota in experimental psoriasis revealed by a gnotobiotic mouse model. *Front Microbiol*. 2019;10:236. doi:10.3389/fmicb.2019.00236
32. Zhao Q, Yu J, Zhou H, et al. Intestinal dysbiosis exacerbates the pathogenesis of psoriasis-like phenotype through changes in fatty acid metabolism. *Signal Transduct Target Ther*. 2023;8(1):40. doi:10.1038/s41392-022-01219-0
33. Chen Y, Song S, Wang Y, Zhu J, Li X. Potential mechanism of oral baicalin treating psoriasis via suppressing Wnt signaling pathway and inhibiting Th17/IL-17 axis by activating PPARγ. *Phytother Res*. 2022;36(10):3969–3987. doi:10.1002/ptr.7546
34. Wang L, Xian Y-F, Loo SKF, et al. Baicalin ameliorates 2,4-dinitrochlorobenzene-induced atopic dermatitis-like skin lesions in mice through modulating skin barrier function, gut microbiota and JAK/STAT pathway. *Bioorg Chem*. 2022;119:105538. doi:10.1016/j.bioorg.2021.105538
35. Yuan X, Li N, Zhang M, et al. Taxifolin attenuates IMQ-induced murine psoriasis-like dermatitis by regulating T helper cell responses via Notch1 and JAK2/STAT3 signal pathways. *Biomed Pharmacother*. 2020;123:109747. doi:10.1016/j.biopha.2019.109747
36. Hou J, Hu M, Zhang L, Gao Y, Ma L, Xu Q. Dietary taxifolin protects against dextran sulfate sodium-induced colitis via NF-κB signaling, enhancing intestinal barrier and modulating gut microbiota. *Front Immunol*. 2020;11:631809. doi:10.3389/fimmu.2020.631809
37. Shabbir U, Rubab M, Daliri EB-M, Chelliah R, Javed A, Oh D-H. Curcumin, quercetin, catechins and metabolic diseases: the role of gut microbiota. *Nutrients*. 2021;13(1):206. doi:10.3390/nu13010206
38. Scazzocchio B, Minghetti L, D'Archivio M. Interaction between gut microbiota and curcumin: a new key of understanding for the health effects of curcumin. *Nutrients*. 2020;12(9). doi:10.3390/nu12092499
39. Li JQ, Zhang S-H, Tong R-S, He D, Zhong Z-D, She S-Y. Curcuma's extraction attenuates propranolol-induced psoriasis like in mice by inhibition of keratin, proliferating cell nuclear antigen and toll-like receptor expression. *Pak J Pharm Sci*. 2020;33(3):1033–1048.
40. Di T, Zhao J, Wang Y, et al. Tuhuaiyin alleviates imiquimod-induced psoriasis via inhibiting the properties of IL-17-producing cells and remodels the gut microbiota. *Biomed Pharmacother*. 2021;141:111884. doi:10.1016/j.biopha.2021.111884
41. Esplugues E, Huber S, Gagliani N, et al. Control of TH17 cells occurs in the small intestine. *Nature*. 2011;475(7357):514–518. doi:10.1038/nature10228
42. McGovern D, Powrie F. The IL23 axis plays a key role in the pathogenesis of IBD. *Gut*. 2007;56(10):1333–1336. doi:10.1136/gut.2006.115402
43. Atarashi K, Tanoue T, Ando M, et al. Th17 cell induction by adhesion of microbes to intestinal epithelial cells. *Cell*. 2015;163(2):367–380. doi:10.1016/j.cell.2015.08.058
44. Ivanov II, Frutos R, Manel N, et al. Specific microbiota direct the differentiation of IL-17-producing T-helper cells in the mucosa of the small intestine. *Cell Host Microbe*. 2008;4(4):337–349. doi:10.1016/j.chom.2008.09.009
45. Atarashi K, Tanoue T, Shima T, et al. Induction of colonic regulatory T cells by indigenous Clostridium species. *Science*. 2011;331(6015):337–341. doi:10.1126/science.1198469
46. Geuking MB, Cahenzli J, Lawson MAE, et al. Intestinal bacterial colonization induces mutualistic regulatory T cell responses. *Immunity*. 2011;34(5):794–806. doi:10.1016/j.immuni.2011.03.021
47. Mazmanian SK, Liu CH, Tzianabos AO, Kasper DL. An immunomodulatory molecule of symbiotic bacteria directs maturation of the host immune system. *Cell*. 2005;122(1):107–118. doi:10.1016/j.cell.2005.05.007
48. Telesford KM, Yan W, Ochoa-Reparaz J, et al. A commensal symbiotic factor derived from Bacteroides fragilis promotes human CD39(+)Foxp3(+) T cells and Treg function. *Gut Microbes*. 2015;6(4):234–242. doi:10.1080/19490976.2015.1056973
49. Palm NW, de Zoete MR, Cullen TW, et al. Immunoglobulin A coating identifies colitogenic bacteria in inflammatory bowel disease. *Cell*. 2014;158(5):1000–1010. doi:10.1016/j.cell.2014.08.006
50. Ivanov II, Atarashi K, Manel N, et al. Induction of intestinal Th17 cells by segmented filamentous bacteria. *Cell*. 2009;139(3):485–498. doi:10.1016/j.cell.2009.09.033
51. Dickson I. Gut microbiota: oral bacteria: a cause of IBD? *Nat Rev Gastroenterol Hepatol*. 2018;15(1):4–5. doi:10.1038/nrgastro.2017.161
52. Chudnovskiy A, Mortha A, Kana V, et al. Host-protozoan interactions protect from mucosal infections through activation of the inflammasome. *Cell*. 2016;167(2):444–456.e14. doi:10.1016/j.cell.2016.08.076
53. Sikora M, Stec A, Chrabaszcz M, et al. Gut microbiome in psoriasis: an updated review. *Pathogens*. 2020;9(6). doi:10.3390/pathogens9060463
54. De Palma G, Lynch MDJ, Lu J, et al. Transplantation of fecal microbiota from patients with irritable bowel syndrome alters gut function and behavior in recipient mice. *Sci Transl Med*. 2017;9(379). doi:10.1126/scitranslmed.aaf6397
55. Scarpa R, Manguso F, D'Arienzo A, et al. Microscopic inflammatory changes in colon of patients with both active psoriasis and psoriatic arthritis without bowel symptoms. *J Rheumatol*. 2000;27(5):1241–1246.
56. Chan HHY, Siu PLK, Choy CT, et al. Novel multi-strain E3 probiotic formulation improved mental health symptoms and sleep quality in Hong Kong Chinese. *Nutrients*. 2023;15(24):5037. doi:10.3390/nu15245037
57. Xiong Q, Li L, Xiao Y, et al. The effect of inulin-type fructans on plasma trimethylamine N-oxide levels in peritoneal dialysis patients: a randomized crossover trial. *mol Nutr Food Res*. 2023;67(9):e2200531. doi:10.1002/mnfr.202200531
58. Huang B, Gui M, An H, et al. Babao Dan alleviates gut immune and microbiota disorders while impacting the TLR4/MyD88/NF-κB pathway to attenuate 5-Fluorouracil-induced intestinal injury. *Biomed Pharmacother*. 2023;166:115387. doi:10.1016/j.biopha.2023.115387
59. den Besten G, van Eunen K, Groen AK, Venema K, Reijngoud D-J, Bakker BM. The role of short-chain fatty acids in the interplay between diet, gut microbiota, and host energy metabolism. *J Lipid Res*. 2013;54(9):2325–2340. doi:10.1194/jlr.R036012
60. Lou Y, Wen X, Song S, et al. Dietary pectin and inulin: a promising adjuvant supplement for collagen-induced arthritis through gut microbiome restoration and CD4+ T cell reconstitution. *J Nutr Biochem*. 2024:109699. doi:10.1016/j.jnutbio.2024.109699.
61. Hamer HM, Jonkers DMAE, Bast A, et al. Butyrate modulates oxidative stress in the colonic mucosa of healthy humans. *Clin Nutr*. 2009;28(1):88–93. doi:10.1016/j.clnu.2008.11.002
62. Smith PM, Howitt MR, Panikov N, et al. The microbial metabolites, short-chain fatty acids, regulate colonic Treg cell homeostasis. *Science*. 2013;341(6145):569–573. doi:10.1126/science.1241165
63. Du X, Yan C, Kong S, et al. Successful secukinumab therapy in plaque psoriasis is associated with altered gut microbiota and related functional changes. *Front Microbiol*. 2023;14:1227309. doi:10.3389/fmicb.2023.1227309

64. De Francesco MA, Caruso A. The gut microbiome in psoriasis and crohn's disease: is its perturbation a common denominator for their pathogenesis? *Vaccines (Basel)*. 2022;10(2). doi:10.3390/vaccines10020244
65. Levy M, Kolodziejczyk AA, Thaiss CA, Elinav E. Dysbiosis and the immune system. *Nat Rev Immunol*. 2017;17(4):219–232. doi:10.1038/nri.2017.7
66. Dokoshi T, Chen Y, Cavagnero KJ, et al. Dermal injury drives a skin to gut axis that disrupts the intestinal microbiome and intestinal immune homeostasis in mice. *Nat Commun*. 2024;15(1):3009. doi:10.1038/s41467-024-47072-3
67. Negi S, Singh H, Mukhopadhyay A. Gut bacterial peptides with autoimmunity potential as environmental trigger for late onset complex diseases: in-silico study. *PLoS One*. 2017;12(7):e0180518. doi:10.1371/journal.pone.0180518
68. Sikora M, Stec A, Chrabaszcz M, et al. Clinical implications of intestinal barrier damage in psoriasis. *J Inflamm Res*. 2021;14:237–243. doi:10.2147/JIR.S292544
69. Gryaznova MV, Solodskikh SA, Panevina AV, et al. Study of microbiome changes in patients with ulcerative colitis in the Central European part of Russia. *Heliyon*. 2021;7(3):e06432. doi:10.1016/j.heliyon.2021.e06432
70. Efremova I, Maslennikov R, Medvedev O, et al. Gut microbiota and biomarkers of intestinal barrier damage in cirrhosis. *Microorganisms*. 2024;12 (3). doi:10.3390/microorganisms12030463
71. Xiang Y, Zhang C, Wang J, et al. Identification of host gene-microbiome associations in colorectal cancer patients using Mendelian randomization. *J Transl Med*. 2023;21(1):535. doi:10.1186/s12967-023-04335-9
72. Song S, Lou Y, Mao Y, et al. Alteration of gut microbiome and correlated amino acid metabolism contribute to hyperuricemia and Th17-driven inflammation in Uox-KO mice. *Front Immunol*. 2022;13:804306. doi:10.3389/fimmu.2022.804306
73. Berry D, Kuzyk O, Rauch I, et al. Intestinal microbiota signatures associated with inflammation history in mice experiencing recurring colitis. *Front Microbiol*. 2015;6:1408. doi:10.3389/fmicb.2015.01408
74. Caruso R, Mathes T, Martens EC, et al. A specific gene-microbe interaction drives the development of Crohn's disease-like colitis in mice. *Sci Immunol*. 2019;4(34). doi:10.1126/sciimmunol.aaw4341
75. Bailén M, Bressa C, Martínez-López S, et al. microbiota features associated with a high-fat/low-fiber diet in healthy adults. *Front Nutr*. 2020;7:583608. doi:10.3389/fnut.2020.583608
76. Kong C, Gao R, Yan X, Huang L, Qin H. Probiotics improve gut microbiota dysbiosis in obese mice fed a high-fat or high-sucrose diet. *Nutrition*. 2019;60:175–184. doi:10.1016/j.nut.2018.10.002
77. Wang B, Kong Q, Li X, et al. A high-fat diet increases gut microbiota biodiversity and energy expenditure due to nutrient difference. *Nutrients*. 2020;12(10):3197. doi:10.3390/nu12103197
78. Kim SJ, Kim S-E, Kim AR, Kang S, Park M-Y, Sung M-K. Dietary fat intake and age modulate the composition of the gut microbiota and colonic inflammation in C57BL/6J mice. *BMC Microbiol*. 2019;19(1):193. doi:10.1186/s12866-019-1557-9
79. Natividad JM, Lamas B, Pham HP, et al. Bilophila wadsworthia aggravates high fat diet induced metabolic dysfunctions in mice. *Nat Commun*. 2018;9(1):2802. doi:10.1038/s41467-018-05249-7
80. Feng Z, Long W, Hao B, et al. A human stool-derived Bilophila wadsworthia strain caused systemic inflammation in specific-pathogen-free mice. *Gut Pathog*. 2017;9:59. doi:10.1186/s13099-017-0208-7
81. Haidmayer A, Bosch P, Lackner A, D'Orazio M, Fessler J, Stradner MH. Effects of probiotic strains on disease activity and enteric permeability in psoriatic arthritis-a pilot open-label study. *Nutrients*. 2020;12(8):2337. doi:10.3390/nu12082337
82. Liu Z, Ma Y, Qin H. Potential prevention and treatment of intestinal barrier dysfunction using active components of Lactobacillus. *Ann Surg*. 2011;254(5):832–833. doi:10.1097/SLA.0b013e318235dd56
83. Chattopadhyay I, Dhar R, Pethusamy K, et al. Exploring the role of gut microbiome in colon cancer. *Appl Biochem Biotechnol*. 2021;193(6):1780–1799. doi:10.1007/s12010-021-03498-9
84. Chen Y-H, Wu C-S, Chao Y-H, et al. Lactobacillus pentosus GMNL-77 inhibits skin lesions in imiquimod-induced psoriasis-like mice. *J Food Drug Anal*. 2017;25(3):559–566. doi:10.1016/j.jfda.2016.06.003
85. Chapat L, Chemin K, Dubois B, Bourdet-Sicard R, Kaiserlian D. Lactobacillus casei reduces CD8+ T cell-mediated skin inflammation. *Eur J Immunol*. 2004;34(9):2520–2528. doi:10.1002/eji.200425139
86. Hacini-Rachinel F, Gheit H, Le Luduec J-B, Dif F, Nancey S, Kaiserlian D. Oral probiotic control skin inflammation by acting on both effector and regulatory T cells. *PLoS One*. 2009;4(3):e4903. doi:10.1371/journal.pone.0004903
87. Chuandong Z, Hu J, Li J, et al. Distribution and roles of Ligilactobacillus murinus in hosts. *Microbiol Res*. 2024;282:127648. doi:10.1016/j.micres.2024.127648
88. Guerrero Sanchez M, Passot S, Campoy S, Olivares M, Fonseca F. Ligilactobacillus salivarius functionalities, applications, and manufacturing challenges. *Appl Microbiol Biotechnol*. 2022;106(1):57–80. doi:10.1007/s00253-021-11694-0
89. Chen R, Xu Y, Wu P, et al. Transplantation of fecal microbiota rich in short chain fatty acids and butyric acid treat cerebral ischemic stroke by regulating gut microbiota. *Pharmacol Res*. 2019;148:104403. doi:10.1016/j.phrs.2019.104403